Speed and direction selectivity of macaque middle temporal neurons

L. Lagae, S. Raiguel and G. A. Orban

J Neurophysiol 69:19-39, 1993.

Journal of Neurophysiology publishes original articles on the function of the nervous system. It is published 12 times a year (monthly) by the American Physiological Society, 9650 Rockville Pike, Bethesda MD 20814-3991. Copyright © 1993 by the American Physiological Society. ISSN: 0022-3077, ESSN: 1522-1598. Visit our website at http://www.the-aps.org/.

JOURNAL OF NEUROPHYSIOLOGY
Vol. 69. No. 1. January 1993. *Printed in U.S.A.*

Speed and Direction Selectivity of Macaque Middle Temporal Neurons

L. LAGAE, S. RAIGUEL, AND G. A. ORBAN
Laboratorium voor Neuro- en Psychofysiologie, Katholieke Universiteit te Leuven, Campus Gasthuisberg, B-3000 Leuven, Belgium

SUMMARY AND CONCLUSIONS

1. We tested quantitatively the responses of 147 middle temporal (MT) cells to light and dark bars moving at different speeds ranging over a 1,000-fold range (0.5–512 deg/s).

2. We derived the following quantities from the speed-response (SR) curves obtained for opposite directions of motion. Speed selectivity was characterized by the maximum response, optimum speed, upper cutoff speed, response to slow movement, and tuning width. Direction selectivity was characterized by the direction index (DI) averaged over speeds yielding significant responses (MDI) and by the direction index at optimal speed (PDI).

3. There was an excellent correlation between speed characteristics for light and dark bars. These correlations were stronger than the correlations between direction indexes. The strongest correlations were obtained for maximum response and upper cutoff.

4. SR curves were classified into three groups: low pass (25%), tuned (43%), and broadband (28%), leaving 4% unclassified.

5. In the majority (75%) of MT cells, there was an agreement between the typology of speed selectivity for light and dark bars. Cells were classified as tuned (33%), low pass (22%), broadband (19%), and mixed (22%), leaving 4% unclassified. In addition to differences in speed characteristics, these groups also differed in response level, direction selectivity, and distribution of preferred directions.

6. For tuned cells, there was a very tight correlation of most speed characteristics for light and dark bars.

7. Direction selectivity depended on stimulus speed in most neurons, yielding a tuned average speed-DI curve.

8. Speed characteristics, proportions of speed selectivity types, and direction selectivity indexes showed little dependence on laminar position.

9. Speed characteristics and direction selectivity indexes were not dependent on eccentricity. Proportion of speed selectivity types however, changed dramatically with eccentricity: low-pass cells dominated foveally, tuned cells parafoveally, and broadband cells peripherally.

10. There were also small eccentricity effects on the range of optimal speeds shown by tuned cells and on the speed at which direction selectivity decreases in the slow speed range.

INTRODUCTION

Ever since its discovery by Dubner and Zeki (1971), the middle temporal (MT) area has been implicated in the analysis of visual motion. Recent evidence (Lagae et al. 1991; Marcar et al. 1991) has shown that MT cells extract local retinal velocity vectors from more complex motion configurations. This in turn implies that MT neurons encode direction and speed of motion in the retina. There is ample evidence concerning the analysis of direction of motion by MT cells. Physiological studies have shown that the overwhelming majority of MT cells are direction selective (Albright 1984; Dubner and Zeki 1971; Maunsell and Van Essen 1983; Mikami et al. 1986a; Movshon et al. 1985; Rodman and Albright 1987; Saito et al. 1989; Zeki 1974) and that there is a columnar organization for direction (Albright et al. 1984). This organization has been confirmed by 2-deoxyglucose experiments (Tootell and Born 1991). Lesion studies have revealed deficits in directional judgements by macaque monkeys after MT lesions (Newsome and Paré 1988), and electrical stimulation of MT interferes with directional judgements in the same species (Salzman and Newsome 1991).

The other parameter of local translation, speed of motion, has received less attention. Yet lesion studies show that, after MT lesions, speed discrimination is severely impaired (Merigan et al. 1991; Vandenbussche et al. 1991), a finding correlated with neuropsychological findings in humans (Plant and Nakayama 1991; Vaina et al. 1991). Thus area MT also seems to contribute heavily to the encoding of retinal speed. Much less is known of the speed selectivity of MT neurons, and the aim of the present paper is to correct this deficiency. Maunsell and Van Essen (1983) reported that the majority of MT cells are tuned for speed, a finding that has also been reported for the awake monkey by Mikami et al. (1986a). However Komatsu and Wurtz (1988) reported that a number of foveal MT cells are active during pursuit in darkness. These authors went on to show that these cells had the same preferred direction for both visual stimuli and pursuit, and that these cells required retinal motion to be activated (Komatsu and Wurtz 1988; Newsome et al. 1988). They concluded that there must be a population of cells with foveal receptive fields (RFs) encoding slow speeds. The first aim of our study was therefore to investigate the effect of eccentricity on speed selectivity of MT cells. In particular, we wanted to investigate whether velocity low-pass cells are present in foveal MT, as they are in the central representation of many cortical areas of cat (Duysens et al. 1982; Orban et al. 1981a) and monkey (Orban et al. 1986). In monkey V1, there is a clear laminar influence on velocity sensitivity (Orban et al. 1986), therefore a second aim was to study such laminar influences in MT. The three previous studies on speed selectivity of MT cells (Maunsell and Van Essen 1983; Mikami et al. 1986a; Rodman and Albright 1987) all used moving light bars, and very little is known about the invariance of velocity sensitivity with changes in stimulus characteristics. Therefore the third aim of the present study was to study the invariance of speed selectivity for changes in contrast polarity that are known to be important for direction and speed selectivity

(Albus 1980; Orban et al. 1987; Yamane et al. 1985). Finally, in the cat cortical areas and in monkey V1, direction selectivity has been shown to depend on stimulus speed and, in particular, to decrease at slow speeds (Duysens et al. 1987; Movshon 1975; Orban et al. 1981b, 1986). Rodman and Albright (1987) reported that, in some MT cells, direction selectivity changed with speed, whereas in others it did not. The final aim of this study was to reinvestigate this issue of great theoretical importance over a wider range of speeds.

METHODS

General procedure

The responses of MT neurons were recorded in 10 anesthetized and paralyzed macaque monkeys (*Macaca fascicularis;* weight, 2.5–5.8 kg). For initial surgical procedures, the animals were anesthetized with a mixture of ketamine and xylazine (Rompun) supplemented by infiltration of surgical areas with a local anesthetic (Xylocaine). The animals were prepared for recording by installation of an intravenous catheter and intubation via tracheotomy. They were then placed in a stereotaxic apparatus with the use of a head-holding device cemented to the skull for the duration of the experiment.

During testing, continuous paralysis was maintained by intravenous infusion of pancuronium bromide ($0.4\ mg \cdot kg^{-1} \cdot hr^{-1}$). General anesthesia was sustained with either one of two regimens with identical results. Animals were either ventilated with N_2O_2:O_2:CO_2 (70:27.5:2.5) and infused with $1\ mg \cdot kg^{-1} \cdot h^{-1}$ of pentobarbital sodium in Ringer–10% glucose, or ventilated with ordinary air containing 2.5% CO_2 and infused with sufentamil citrate (Sufenta Forte) ($5\ \mu g \cdot kg^{-1} \cdot hr^{-1}$) in Ringer-glucose. Vital signs, including heart rate, rectal temperature, and end expiratory CO_2, were monitored continuously. In some animals arterial blood gas measurements were used to adjust the ventilatory settings. The broad-spectrum antibiotic cefazolin was administered intramuscularly each day, and all surgical wounds were treated with virginiamycin-neomycin powder (Spitalen). Corneas were protected with a focal conflex contact lenses and refraction errors corrected with spectacle lenses. Frequent back projection of the fovea and optic disk corrected for eye drift during the course of the experiment. Pupils were dilated with topically applied atropine, and the optics kept clear by daily cleaning under local anesthetic and by applying antibiotic drops (Spitalen pro instillatione).

To obtain recordings, a 1 × 1–cm craniotomy was performed over the dorsolateral surface of the skull, and an electrode was inserted through a small slit made in the dura just between the superior temporal and lunate sulci, and ~15 mm laterally. Electrodes were of glass-coated tungsten with an exposed tip of 8 μm. The electrode was angled rostrally, in the sagittal plane, at 25–35° from the vertical. This approach runs nearly parallel to the strip of cortex in the superior temporal sulcus containing MT and has several advantages. It results in long tracks within the same lamina, permitting easy reconstruction of those tracks, and it produces a higher yield of units in the thinner, deep layers, so that our sampling is relatively equal throughout the laminae. Also, the angle of the approach generally gives a steady progression of visual fields from peripheral to foveal, evenly sampling cells at all eccentricities. During the course of each penetration, several electrolytic lesions were made to facilitate histological reconstruction of the track. After 5 days of recording, the animals were killed with pentobarbital and the brains perfused with buffered Formalin. Alternate 60-μm frozen sections were stained with cresyl violet and myelin stain (Gallyas 1979). MT borders were determined from the myelin sections, according to the criteria of Van Essen et al. (1981), and the cresyl violet sections were used for reconstruction of the track and laminar position. Because layers 2 and 3 are histologically indistinguishable and functionally similar, no attempt was made to differentiate these laminae.

Units were initially hand plotted on a plotting table 86 cm from the animal, with the use of small hand-held stimuli (Orban and Kennedy 1981). In this way, we obtained qualitative assessments of such properties as the position and extent of the RF, preferred orientation axis, orientation tuning width, binocularity, and degree of end stopping of the cell. The coordinates of the RF were then transferred to a Polacoat screen located 1.71 m in front of the monkey for quantitative testing of cell properties. Only the eye giving the strongest response was used in these tests, with a shutter occluding the opposite eye.

Two projectors were used to provide the stimuli, which were back projected onto the Polacoat screen. Rotating mirrors driven by scanning galvanometers (G.300 PD, General Scanning) controlled the movement and speed of the stimulus, an electronic shutter limited the duration, and stepper motor-driven neutral density wedges adjusted the contrast. These devices were in turn under control of the STIMUL program (Maes and Orban 1980) running on the PDP-11, which handled the details of stimulus movement and timing, spike event recording and synchronization and provided on-line, cumulative, peristimulus time histograms (PSTHs) of spike activity. The projectors contained a light and a dark bar of equal contrast but opposite in polarity (Yamane et al. 1985), with a background luminance of $4.9\ cd/m^2$ and a contrast ($\log \Delta I/I$) of −0.09. In all other respects, the light and dark stimuli were completely identical. Bar speed normally ranged from 0.5 to 512 deg/s, although, in a number of cells, speeds as slow as 0.25 or even 0.13 deg/s were used. These changes in speed were obtained by manipulating the spatial (Δx) or temporal (Δt) increments of the mirror position. At 16 deg/s the Δx was 1 min of arc and Δt 1 ms. Slower speeds were obtained by increasing Δt and faster speeds by increasing Δx. At all speeds, motion looked smooth to the human observer. The length and width of the bars used were optimal for the cell as determined by hand plotting, and the sweep length and starting position were always adjusted so that movement began and ended outside the visual field. Every speed was presented in both the forward and the reverse direction along the optimal axis. The 2 directions, 2 polarities, and 11 speeds yield a total of 44 conditions, which were presented for each cell tested. Each of the 44 conditions was presented ~8–12 times, in a pseudorandomized order, until the on-line PSTHs showed that a clear response was present.

Throughout our analysis, we have used maximum firing rate (MFR) as a response measurement, that is, the 32-ms bin containing the maximum number of spikes during the period of stimulation. Preliminary analysis has shown that a binwidth of 32 is a satisfactory compromise between larger binwidths, which underestimate speed upper cutoff, and lower binwidths, which give small signal-to-noise ratios (Fig. 1). The choice of binwidth had no significant effect on other speed parameters, such as response to slow, and thus did not affect the distinction between tuned and low-pass curves (Fig. 1). The binwidth of 32 ms used in the present study is a factor 4 larger than those used in previous studies from this laboratory. This is related to the large width of MT RFs. Indeed, because of this large width compared, e.g., with that of V1 RFs, the shortest response duration, obtained at fast speeds, exceeded 65 ms, thus justifying the use of a 32-ms binwidth. Each stimulus presentation was preceded by a 250-ms period during which there was no visual stimulation (prestimulus period). The mean and standard deviation of the MFRs of the 44 cumulative prestimulus histograms provided a measure of the spontaneous activity of the cell. A response was then considered significant if it exceeded the mean plus twice the standard deviation of the maximum spontaneous firing rate.

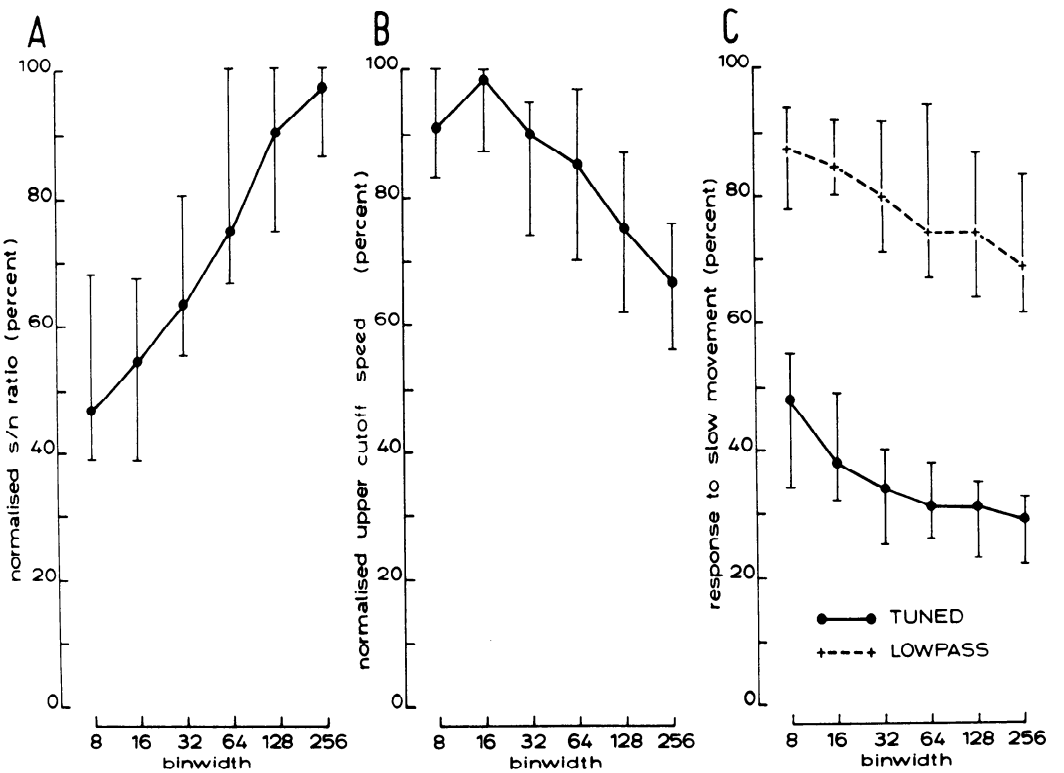

FIG. 1. Influence of binwidth on response and speed characteristics. *A*: signal-to-noise ratio plotted as a function of binwidth. Signal-to-noise ratio is defined as the ratio between the maximum response obtained in the speed-response curve and the spontaneous maximum firing rate. Ratios at the different binwidths were normalized for each cell by taking the largest ratio for each cell as 100%, and the median and quartiles are shown for each binwidth ($n = 19$). *B*: upper cutoff speed as a function of binwidth for tuned cells ($n = 19$). Upper cutoff speeds were normalized for each cell, and median and quartiles are shown. *C*: response to slow movement as a function of binwidth for tuned cells ($n = 19$) and low-pass cells ($n = 14$). Median and quartiles are depicted. A change in binwidth does not affect our speed selectivity classification: the average response to slow movement remained >60% for the low-pass cells, and <50% for the tuned cells.

Direction and speed characteristics

For each speed, a direction index (DI) was calculated according to the formula $DI = (1 - R_{np}/R_p) \times 100$, where R_p is the significant response in the preferred direction (PD) and R_{np} is the significant response in the reverse, or nonpreferred direction (NPD). The significant response equals the response to the stimulus minus the mean and twice the standard deviation of the spontaneous firing rate. No DI was calculated at speeds giving no significant response. Because direction selectivity depends on speed (Orban et al. 1986), a mean direction index (MDI) was defined as the weighted average of the direction indexes for all the speeds tested. The significant responses in the PD were used as weighting factors, thus giving most weight to those speeds where the response is highest. Although we believe that this method gives the best overall representation of the direction selectivity of the cell, we also calculated the peak direction index (PDI) for purposes of comparison. This method simply takes the DI at a single point, the speed at which the maximum response for the cell occurs.

The speed-response (SR) curve presents the MFRs from the multihistograms plotted as a function of speed. The curve fitted to these points consists of a third-order spline function through the data points after smoothing the points by the function $R_n = [2R_n + (R_{n-1}) + (R_{n+1})]/4$, where R_n is the response at a given point and R_{n-1} and R_{n+1} are the responses at the preceding and following point, respectively (Figs. 2 and 5). Each cell was characterized by four separate curves, representing the light and dark bar responses in the PD and NPDs. Speed characteristics (see following paragraph) were extracted from the curves for the PD, except in the few instances where the absolute value of the MDI was <33, in which case the mean value for the two curves in opposite directions was used. Where units respond about equally well to opposite directions, this averaging should yield more reliable estimates of the speed characteristics.

Five speed characteristics were extracted from the SR curves: maximum response, optimal speed, upper cutoff, speed response to slow, and tuning width (Fig. 2). The maximum response (2a) is simply the highest point on the curve minus the mean spontaneous activity. The optimal speed (S_2) is the speed corresponding to the highest point of the curve. The upper cutoff speed is the higher of the two speeds (S_1 and S_3) giving one-half the maximum response. Response to slow movement (100 b/2a) is the response to the slowest speed tested, expressed as a percent of the maximum response. The ratio of the upper and slower speeds giving one-half the maximum response defines the width of speed tuning. Thus maximum response and tuning width represent the unit's responsiveness and selectivity for speed respectively. The upper cutoff indicates how well the unit follows fast speeds. Because in many cells no lower cutoff (S_1 in Fig. 2) could be determined, we preferred to use response to slow as measure of responsiveness to slow speeds.

RESULTS

Data base and qualitative observations

One hundred forty-seven MT neurons were tested quantitatively. Histological reconstruction not only confirmed their location within MT but also allowed the recovery of

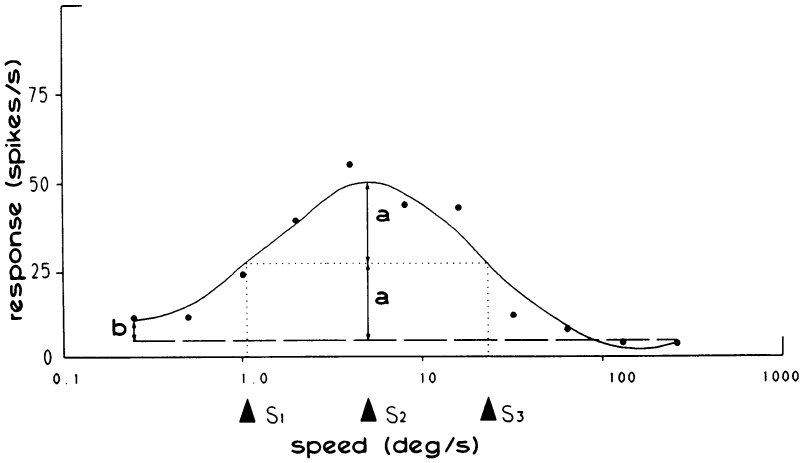

FIG. 2. Definition of speed characteristics: speed-response curve for light bar moving in the preferred direction of *cell 3110*, recorded in layer 5 at an eccentricity of 4°. Horizontal dashed line indicates mean spontaneous activity. Optimal speed (S_2) of this cell was 5 deg/s, and the maximum response (2a) was 42 spikes/s. The upper cutoff speed (S_3) was 16 deg/s, and the response to slow (100 b/2a) was 8%. The tuning width (S_3/S_1) was 18, and the curve was classified as tuned.

their laminar position. Because of the use of penetrations largely parallel to the cortical surface and starting 1–2 mm behind the lumen of the superior temporal sulcur (STS), the number of cells taken in each layer is roughly equal, thus in effect oversampling deep layers: 43 cells were located in layers 2–3, 39 cells in layer 4, 33 in layer 5, and 32 in layer 6. One-half of the cells (74/147) had their RF within the foveal and parafoveal region of MT (0–6° eccentricity). The maximum eccentricity present in the sample was 23°. The complete distribution of the sample in terms of eccentricity and laminar position is given in Table 1.

Eighty-seven cells were best driven by long bars, thus 30° long bars were used for quantitative testing. Shorter bars (median, 3°) were used in the other 60 cells. There was no clear relationship between cells preferring short lengths and eccentricity. Zeki (1974) has previously described a class of neurons in the posterior bank of STS selective for width and length of the stimulus. Maunsell and Van Essen (1983) found an incidence of 3/18 cells with clear end stopping. The foveal MT cells responding during smooth pursuit in the study of Komatsu and Wurtz (1988) all preferred small spots and slits. Thus it is not surprising that a substantial fraction of MT cells in our study were sensitive to the length of the bar. In contrast, the width of the bars was less crucial in obtaining optimal responses, and the standard width used was 0.6°, although 0.3 and 1° wide bars were occasionally used.

The majority of the cells were binocular: 83% of the cells belonged to the ocular dominance classes 3, 4, or 5 as defined by Hubel and Wiesel (1968). This corresponds closely to the 79% in the study of Maunsell and Van Essen (1983). However, quantitative testing was done monocularly with stimuli presented to the dominant eye. All but three cells were clearly directionally tuned, and the optimal axis of motion was used for quantitative testing.

TABLE 1. *Distribution of neurons as a function of eccentricity and layer*

	Eccentricity Class				
Layers	0–3°	3–6°	6–9°	>9°	Total
2–3	2	15	18	8	43
4	8	17	8	6	39
5	13	12	4	4	33
6	1	6	11	14	32
Total	24	50	41	32	147

Changes in speed and direction characteristics with stimulus polarity

As previously mentioned, almost all (143/147) neurons responded to both moving light and dark bars. In these cells we systematically compared the characteristics of the SR curves and the two direction indexes for light and dark bars. There was a very strong correlation between the maximum response for light and dark bars (Fig. 3*A*). The correlation coefficient was 0.91, and the resulting linear regression line was virtually a diagonal. The median maximum response was 47 spikes/s for the dark bar, and 41 spikes/s for the light bar. Among the different speed characteristics, the strongest correlation was obtained for the upper cutoff speed (Fig. 3*B*). Here the correlation coefficient was 0.81, and the line fitted to the data was again very close to a diagonal. Median values for light and dark bars were once more very similar (66 and 54 deg/s, respectively). For response to slow, the correlation was weaker ($r = 0.7$), and the line fitted to the data deviated somewhat from the diagonal (Fig. 3*C*). Indeed, in a number of cells, the response to slow was stronger for one polarity than for the other. Still, the median values for light and dark bars were relatively similar (48 and 56%, respectively). The correlation for optimal speed ($r = 0.69$) was as strong as for response to slow. That the correlation is weaker for optimal speed than for upper cutoff speed is not surprising, because optimum speed is clearly defined only for tuned cells. Considering only these latter cells gives a clearer correlation between values for light and dark bars (see below).

Similar comparisons were made for the direction indexes, the MDI and the PDI. Naturally, the absolute values of these indexes were used in light and dark bars comparisons, because the PD was generally the same for the two polarities. Negative values are used only to indicate that the PD for one polarity was opposite to that of the other. If spatiotemporal interactions between ON and OFF subregions were to underlie the direction selectivity, a different DI would be expected for light and dark bars. Figure 4 shows that this is not the case: for the majority of cells, the

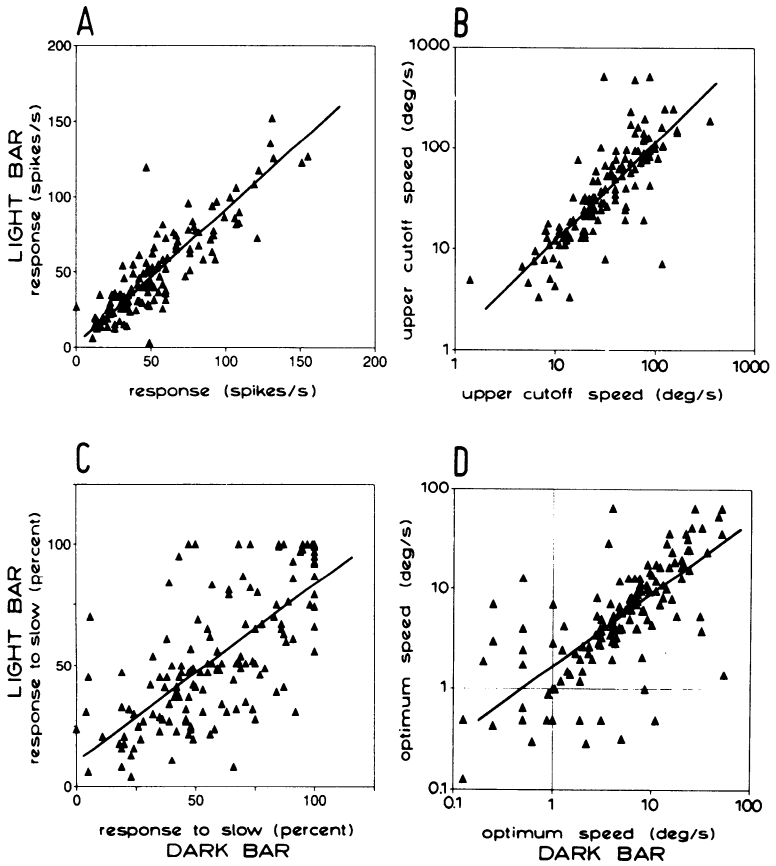

FIG. 3. Comparison of speed characteristics for light and dark bars. *A*: maximum responses. *B*: upper cutoff speeds (log scale). *C*: response to slow. *D*: optimum speed (log scale). Correlation coefficients (r) are 0.91 (*A*), 0.81 (*B*), 0.7 (*C*), and 0.69 (*D*). Equations of linear regressions: $y = 2.1 + 0.89x$ (*A*), $y = 0.13 + 0.96x$ (*B*), $y = 12 + 0.7x$ (*C*), and $y = 0.26 + 0.7x$ (*D*).

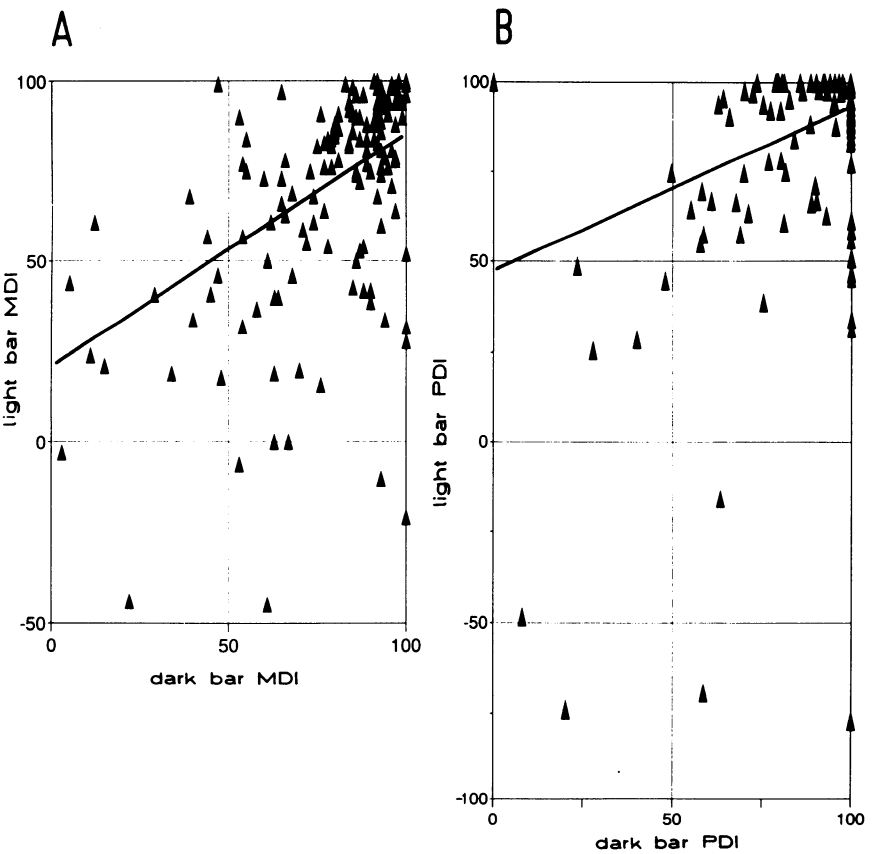

FIG. 4. Comparison of direction selectivity for light and dark bars. *A*: mean direction index (MDI). *B*: peak direction index (PDI). Correlation coefficients were 0.52 (*A*) and 0.46 (*B*). Equations of linear regressions were $y = 22.5 + 0.64x$ (*A*) and $y = 45 + 0.47x$ (*B*). In *A*, the stippled lines indicate MDI = 50, the level below which cells are considered nondirection selective.

MDI was similar for the two polarities. In fact, over three-quarters of the cells (110/143, 77%) had an MDI >50 for dark and light bar, meaning that these average response over the entire range of speeds was at least twice as strong in the PD as in the NPD for either bar. Twenty-one cells in our sample had an MDI exceeding 50 for only one polarity, whereas 11 cells showed little direction selectivity for either bar (MDI <50 for both bars). Only seven cells had a weak preference for opposite directions of dark and light bars, and of these none had MDIs exceeding 50 in absolute value for the two polarities. Although fewer cells had preferences for opposite directions of dark and light bar when PDI was used as measure of direction selectivity, two of these five cells had PDIs exceeding 50 in absolute value for the two polarities. That the correlation between light and dark bars was somewhat weaker for the PDI than for the MDI might be due to a ceiling effect for the PDI. It is noteworthy that, although direction selectivity is relatively invariant with respect to polarity changes, speed characteristics, in particular upper cutoff, and the response level, are much more so.

The two other quantitative studies devoted to direction selectivity in the paralyzed monkey (Albright 1984; Maunsell and Van Essen 1983) used only light bars. In our sample 110/143 (77%) cells had an MDI exceeding 50 for the light bar, and 132/143 (92%) had a PDI exceeding 50. This compares well with the percentage observed in the other two studies: in Maunsell and Van Essen's study 86% of the cells had a DI >50, and, from Fig. 13 in Albright's study, a proportion of 85% can be derived. The comparable value for our study, the PDI, although very close to these values, is slightly different, probably due to the fact that in these former studies the DI was measured at only one speed that was not necessarily the optimal speed. Because the speed and direction characteristics correlate so well for light and dark bars, we will use the averaged value for light and dark bars as characteristic of the neuron. These averaged values will be used in describing the functional architecture of MT (see below).

Speed selectivity types

As mentioned, almost all neurons responded to both contrast polarities. In fact, all neurons were driven by dark bars, and only four cells failed to give significant responses

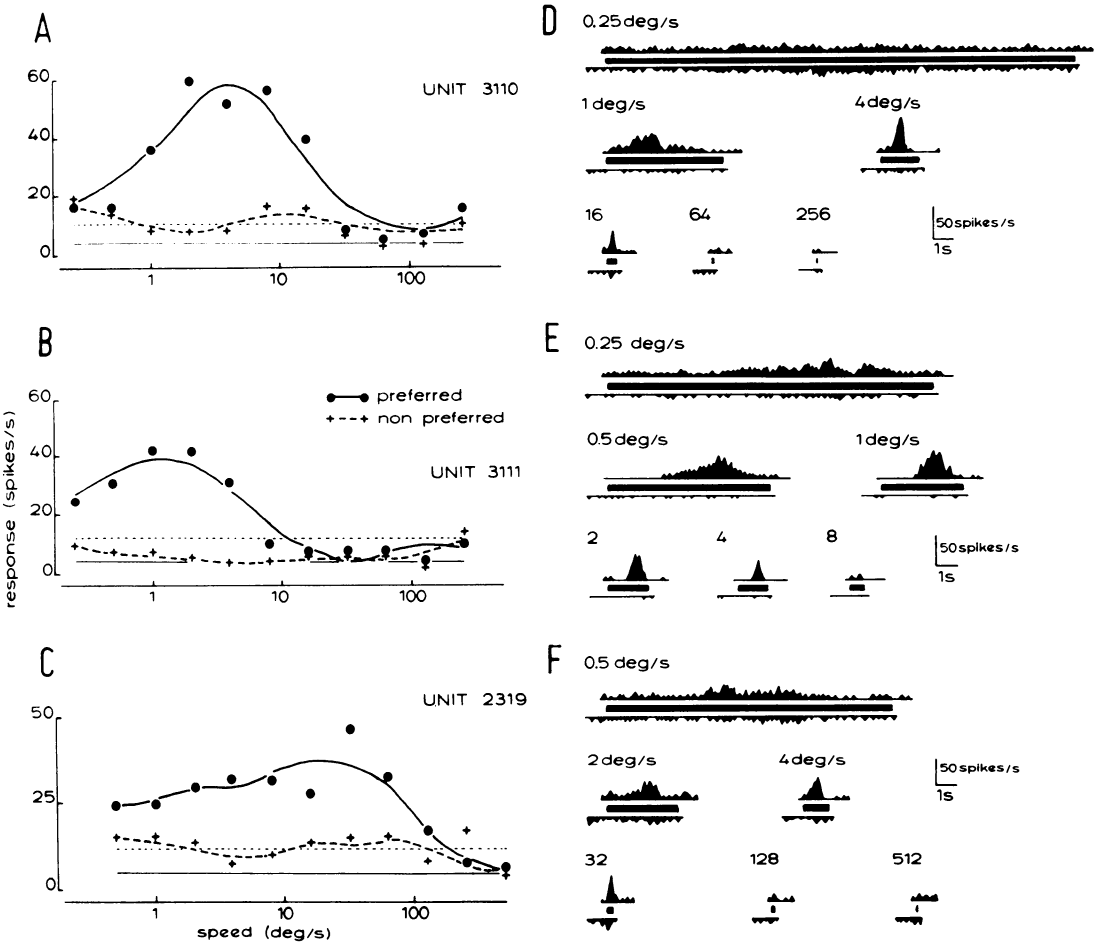

FIG. 5. Examples of the 3 speed-response curves: tuned (*A*), low pass (*B*), and broadband (*C*). *D–F*: peristimulus time histograms (PSTHs) show average responses at selected speeds. In *A–C* the response in preferred direction (PD; ●) and nonpreferred direction (NPD; +) is plotted as a function of speed together with the spline function fitted to the data points (solid line, PD; stippled line, NPD). Horizontal solid line indicates the mean spontaneous activity, and stippled horizontal line the significance level. In *D–F* the PSTHs of the PD are plotted upright and those of the NPD inverted. Horizontal thick line indicates motion duration. Calibration bars are indicated. *Cell 3110* and *3111* were recorded in layer 5 and *cell 2319* in layer 4. Notice that *cells 3110* and *3111* were explored with the speed range shifted down to 0.25 deg/s, whereas *cell 2319* was tested with the standard range.

to the light bar. Thus, in total, 290 SR curves were obtained. Most of these curves followed patterns we have described previously as velocity tuned, velocity low pass, and velocity broadband (Orban et al. 1981a, 1986). Figure 5 illustrates each of these types. *Cell 3110* (Fig. 5*A*) responded to only 5 of the 11 speeds tested, with a clear preference for the 2- to 8-deg/s range. This cell was narrowly tuned for speed, as witnessed by a small tuning width of 18. Thus this cell fits the description of velocity tuned. *Neuron 3111* (Fig. 5*B*) also responded to only a few speeds (5 out of the 11 tested), but all these speeds were slow speeds, and the response to each of these was relatively similar. This behavior is typical of the velocity low-pass cells. Finally *neuron 2319* (Fig. 5*C*) responded over a wide range of speeds because it gave significant responses to 9 of the 11 speeds tested and the SR curve has no clear optimum. Such a behavior fits the description of velocity broadband curves.

The vast majority (121/147) of cells, as *cell 2319* (Fig. 5*C*), were tested with speeds ranging from 0.5 to 512 deg/s. Although this means that we systematically explored speed over a 1,000-fold range, one could argue that the restriction of the range of speeds would affect attribution of SR curves

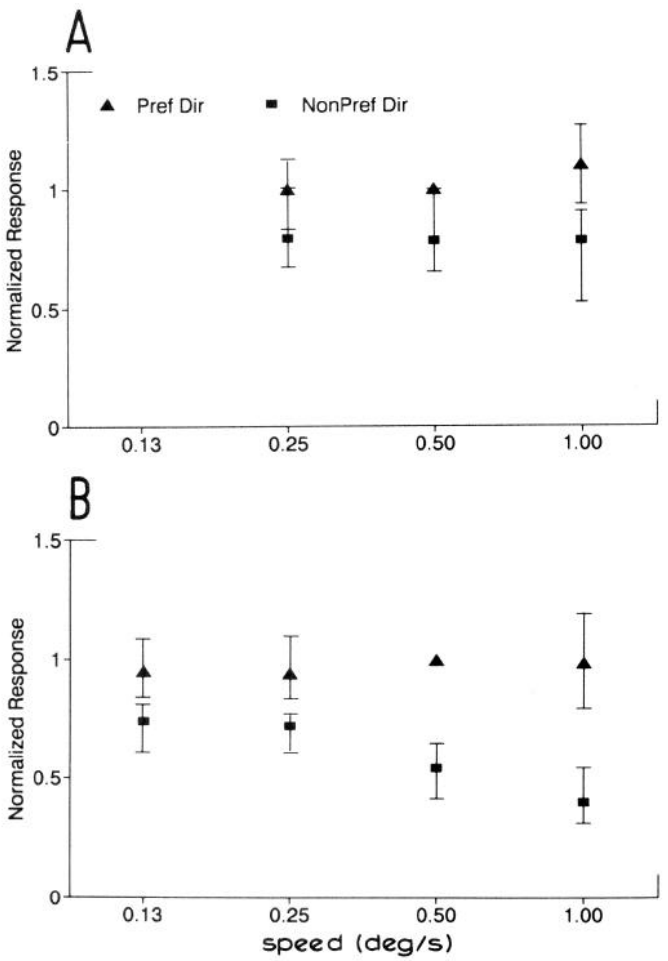

FIG. 6. Median normalized responses to bars moving slowly in preferred direction (PD) and nonpreferred direction (NPD). *A*: sample of 21 cells tested down to 0.25 deg/s. *B*: sample of 8 cells tested down to 0.13 deg/s. Responses were normalized with respect to the response to 0.5 deg/s in the PD. Triangles indicate responses in the PD, and squares, responses in the NPDs. Error bars indicate 1st and 3rd quartiles.

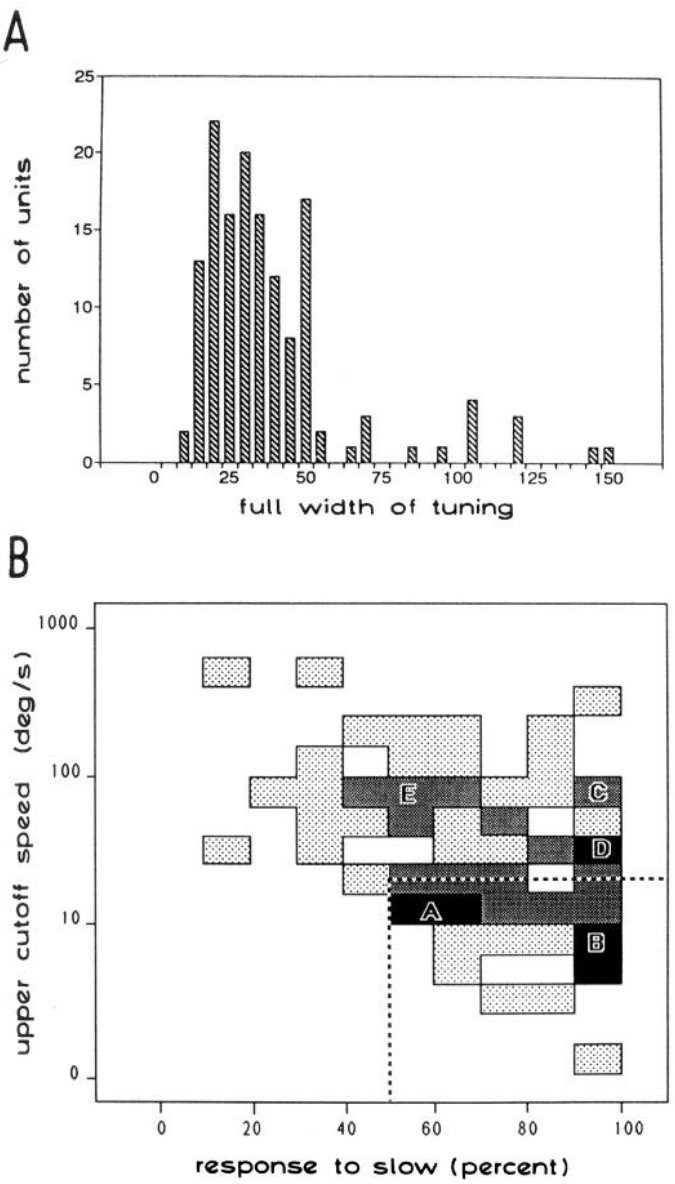

FIG. 7. Distribution of speed-response curves. *A*: distribution of tuning widths for 143 curves for which this characteristic could be measured. *B*: density plot of curves with tuning width exceeding 50 (n = 153) as a function of upper cutoff speed and response to slow. Rectangular bins correspond to 0.2 log unit upper cutoff velocity and 10% response to slow. Light, intermediate, and dark hatching corresponds to 3 levels of density: 1–3, 4–5, and 6–9 curves per rectangle, respectively. Notice the prominent peak in *A* made by curves with tuning width <50: these curves were classified as tuned. The distribution in *A* corresponds much more closely to a normal distribution (Kolmogorov-Smirnov test, $P < 8.7\ 10^{-6}$) than to a γ distribution ($P < 0.03$). Stippled rectangle in *B* marks the definition of low-pass curves: response to slow exceeding 50 and upper cutoff <20 deg/s. Letters A–E indicate peaks in the distribution.

to one of the three above-described types. In particular, one could argue that the distinction between tuned and low-pass cells will vanish if one explores slow enough speeds, because at these slow speeds the responses of all cells, including low-pass cells, would decrease. To rule out this possibility we explored speeds slower than 0.5 deg/s in a number of cells. In 21 cells responding best to slow speeds, we shifted the range downward and tested speeds from 0.25 to 256 deg/s. This showed that in many cells the response in

the PD, as in Fig. 5*A*, does not further decrease at slow speeds. To quantify this effect, we took as reference the response to 0.5 deg/s in the PD, because this response was significant in all cells, and because 0.5 deg/s was the slowest speed tested in most other cells. We expressed all responses from 0.25 and 1 deg/s, in both PD and NPD, as a function of this reference. The results are shown in Fig. 6*A*. Clearly, responses of MT cells were on average equal at all three speeds in the PD. In another 8 cells, still slower speeds were explored by including 0.13 deg/s, either by shifting the 11-speed range downward from 0.13 to 128 deg/s or by testing the 4 slowest speeds (0.13–1 deg/s) separately. The same normalization was performed, with the use of the response to motion at 0.5 deg/s in the PD as the reference (Fig. 6*B*). The outcome of this additional testing confirmed that there is on average little change in the responses to the PD between 0.13 and 1 deg/s. In the NPD there was a gradual increase in response as speed decreased, demonstrating that in these cells direction selectivity decreases at slow speeds, a point that will be taken up later. In conclusion, exploring only speeds of 0.5 deg/s and above will not distort the classification of SR curves. That responses in the PD change little at slow speeds is not really surprising, because at these speeds the local factors of motion [as opposed to sequential factors (Orban 1986)] dominate the SR curve.

To investigate how distinct the different types of SR curves are, we studied the distribution of speed characteristics in the sample of 290 SR curves obtained with either light or dark bar. Ten curves were not considered, either because the response was too weak (8 curves) or because the curves resembled high-pass (Orban et al. 1981a) curves (2 curves). These curves were left unclassified. In Fig. 7*A* the distribution of tuning width is plotted for the 143 out of 280 curves for which this characteristic could be calculated.

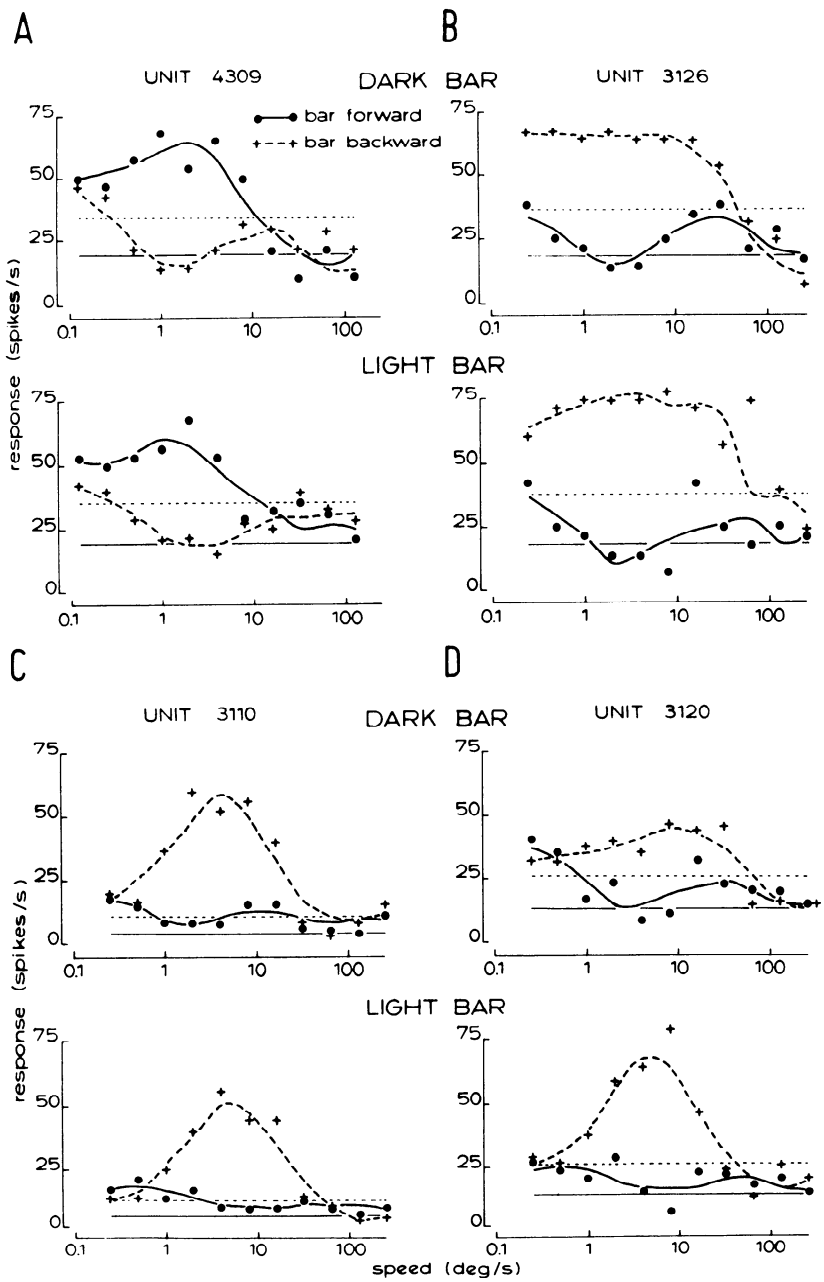

FIG. 8. Examples of the 4 types of middle temporal neurons: low pass (*A*), broadband (*B*), tuned (*C*), and mixed (*D*). Speed-response curves for forward and backward direction are shown. Same conventions as Fig. 5. Cells were recorded in layers 2–3 (*4309*), layer 4 (*3126*), and layer 5 (*3110* and *3120*). Notice that these cells were tested with the range of speeds shifted down to 0.25 deg/s (*B–D*) and to 0.13 deg/s (*A*).

TABLE 2. *Speed selectivity types: comparison of light and dark bars*

Dark Bar	Light Bar LP	BB	TU	UC	NL	Total
LP	31	3	4	0	1	39
BB	1	28	17	0	0	46
TU	2	5	46	2	3	58
UC	0	0	0	4	0	4
Total	34	36	67	6	4	147

LP, low pass; BB, broadband; TU, tuned; UC, unclassified; NL, no response to light bar.

It should be stressed that, with the exception of two curves, the failure to calculate a tuning width was due to the inability to obtain a lower cutoff speed. From the results reported in the previous section (Fig. 6), it follows that this would not change, even if we were to extend the range of speeds tested to slower speeds. There is a clear peak in the histogram of Fig. 7*A*, showing that a large fraction (125/143) of MT SR curves was narrowly tuned for speed, i.e., had a tuning width <50. This value is therefore taken as the defining characteristic of a tuned curve. In Fig. 7*B* the joint distribution of upper cutoff and response to slow is plotted for 153 of the 155 remaining, i.e., nontuned, SR curves. For two curves, upper cutoff speed could not be determined, and these curves were not considered. Several peaks are apparent in the plot of Fig. 7*B*: three peaks, labeled *B*, *C*, and *D*, at high response to slow; and two peaks, A and E, at lower response to slow. The two peaks A and B fall within the area of definition of velocity low-pass curves, which were defined (Orban et al. 1981*a*) as having an upper cutoff <20 deg/s and a response to slow >50%. Because these criteria segregate peaks A and B relatively well from the three remaining peaks, we accept them as defining characteristics for MT low-pass SR curves. Seventy-three curves met this definition, and the remaining (n = 82) were classified as broadband curves. Although the data do not provide evidence for a clustering into discrete classes of speed selectivity, neither do they argue against the criteria previously used in our laboratory. Therefore we have also adopted these criteria for the definition of speed selectivity classes for this study, while recognizing that they are arbitrary and are used only for convenience.

Invariance of the speed selectivity types with contrast polarity

In the majority of neurons (77%), SR curves were of the same type for light and dark bars. This is illustrated in Fig. 8. *Cell 4309* (Fig. 8*A*) was recorded in the superficial layers and had a marked preference for slow speeds. Its speed selectivity was explored with the slowest range, including 0.13 deg/s. The SR characteristics were very similar: the upper cutoff was 8 deg/s for both bars, and the response to slow 64 and 79% for dark and light bar, respectively. The two curves were classified as low pass. *Neuron 3110* (Fig. 8*C*), recorded in layer 5, was clearly tuned for both light and dark bars. Tuning width was 19 and 18 for dark and light bar, respectively. Thus the two curves for this cell were classified as tuned. *Neuron 3126* (Fig. 8*B*), recorded in layer 4, responded over a wide range of speeds. The upper cutoff was 40 and 50 deg/s for dark and light bar, respectively. The response to slow was 100 and 79 for dark and light bars, respectively. Thus both curves fell in the broadband category. Notice that, especially for the dark bar, it is extremely difficult to designate an optimal speed.

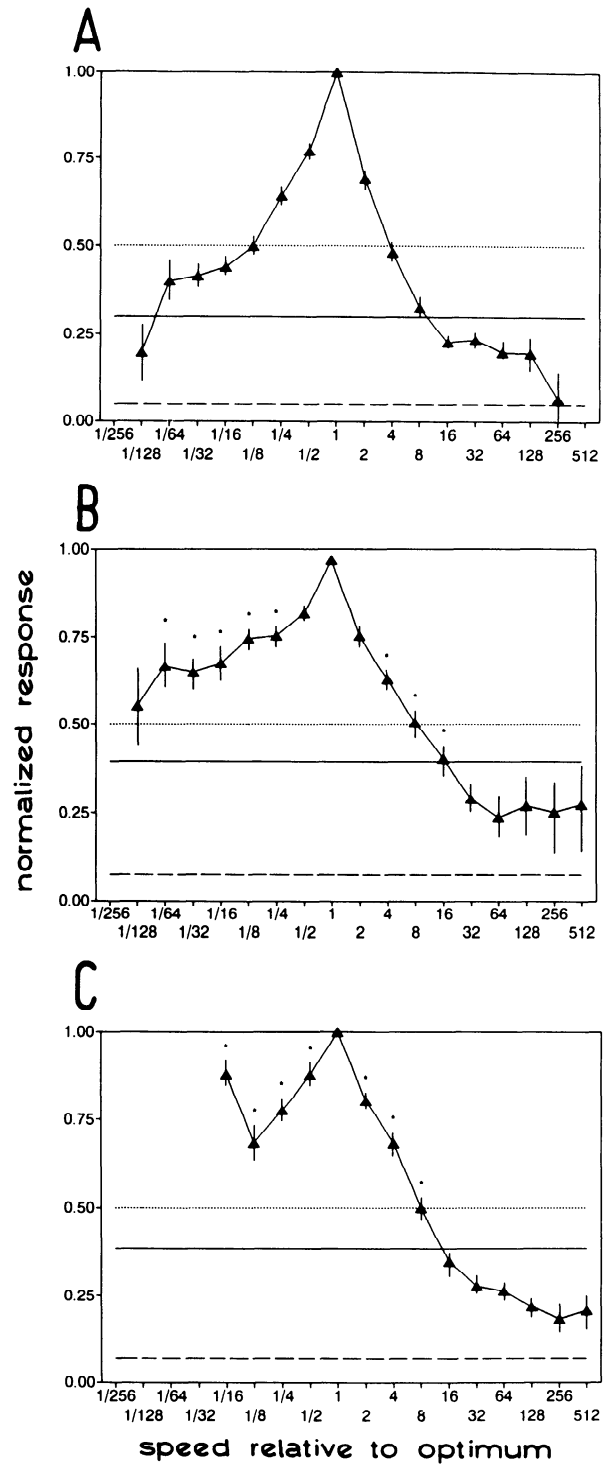

FIG. 9. Average tuning of the 3 types of neurons: tuned (*A*, n = 49), broadband (*B*, n = 28), and low pass (*C*, n = 32). Vertical lines indicate SE. Small asterisks indicate relative speeds at which the curves differed significantly from that of the tuned cells.

TABLE 3. *Speed characteristics of speed selectivity types*

Characteristic Type	Response to Slow, %	Upper Cutoff Speed, deg/s	Optimal Speed, deg/s
Low pass	78 (70–93)	11.4 (7.3–14)	1.7 (1.1–2.4)
Broadband	62 (54–87)	55.6 (36.5–81.8)	7.3 (3.3–12)
Tuned	33 (24–41)	45.7 (28.2–92.3)	9.1 (4.5–14.3)
Mixed	53 (46–62)	33.5 (22.9–53.1)	5.8 (3.9–9.9)
All	53 (37–75)	35.5 (16.4–71)	5.3 (2.4–10.2)

Values shown are median; numbers in parentheses are ranges.

Although the majority of cells behaved as the three cells just described, in a number of cells the speed profiles were different for the two bars. *Cell 3120* (Fig. 8*D*), recorded in layer 5, had a higher upper cutoff for dark bar (50 deg/s) than for light bar (20 deg/s). The response to slow was even more different: 58% for the dark bar compared with 24% for the light bar. Although the dark bar SR curve was classified as broadband, the light curve was clearly tuned.

A comparison of speed profiles for light and dark bars is given in Table 2. In the large majority of the cells with classifiable curves (105/137, 77%) the types of curves matched. The most common dissimilar pairing (n = 22) was a tuned curve combined with a broadband curve as exemplified in Fig. 8*D*. In another six cells the curves for the two polarities were low pass and tuned, and in four cells a low-pass curve was associated with a broadband curve. The tuned curves are distinguished from the other two types by the response to slow. Thus the involvement of many tuned curves in dissimilar pairs (28/32 pairs) reflects the somewhat weaker correlation of response to slow between light and dark bars compared with upper cutoff speed. Given the similarity of speed profiles for the two polarities, cells were classified as tuned, low pass, or broad-

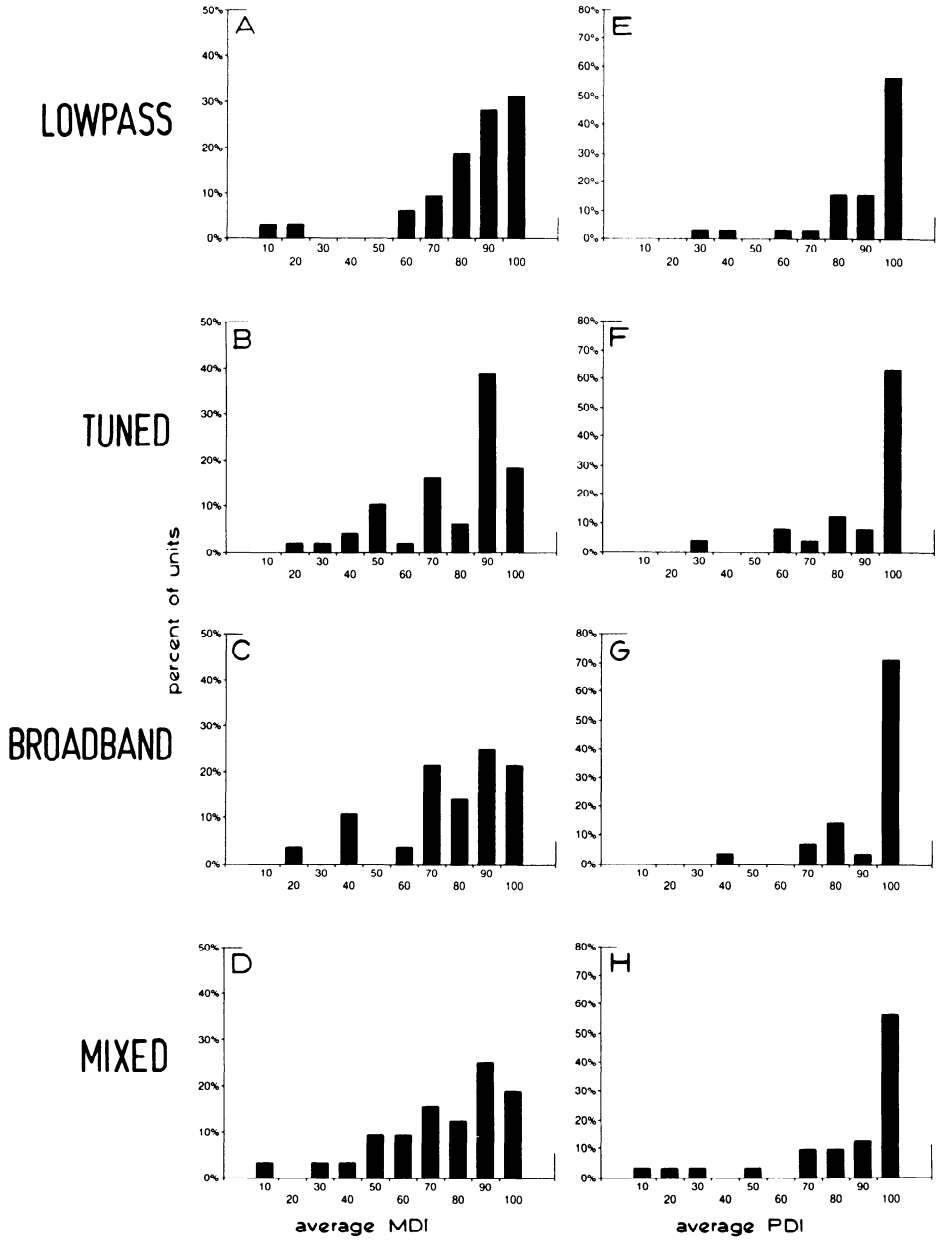

FIG. 10. Direction selectivity of the 4 speed selectivity types: low pass (*A* and *E*), tuned (*B* and *F*), broadband (*C* and *G*), and mixed (*D* and *H*). Distributions of mean direction index (MDI) (*A–D*) and peak direction index (*E–H*) averaged for light and dark bars are plotted.

band if both curves were of the same type, and the remaining cells were labeled mixed. The few cells that responded only to one polarity were classified according to this SR curve for that polarity. In total we classified 49 (33%) cells as tuned, 32 (22%) as low pass, 28 (19%) as broadband, leaving 6 (4%) unclassified and 32 (22%) mixed.

Characteristics of speed selectivity types

As one could expect from the definition of the SR curves, the speed selectivity types differed strongly in speed characteristics, including those not used in the definition of the types. Table 3 gives the average values for the four speed selectivity types. Low-pass cells were characterized by a large response to slow and small upper cutoff speed and optimal speed. Broadband cells were characterized by a large response to slow and large upper cutoff and optimal speeds. Tuned cells typically had small responses to slow and fast upper cutoff and optimal speeds. The differences in response to slow between the tuned cells on one hand and the low-pass and broadband cells on the other hand were very significant ($z = 6.26$, $P < 3.9\ 10^{-10}$ and $z = 7.52$, $P < 5.6\ 10^{-14}$, respectively). Also the differences in upper cutoff and optimal speed between the low-pass cells on one hand and the tuned ($z = 6.98$, $P < 3.1\ 10^{-12}$ and $z = 6.75$, $P < 1.45\ 10^{-11}$, respectively) and broadband cells ($z = 6.57$, $P < 5\ 10^{-11}$ and $z = 4.59$, $P < 4.5\ 10^{10-6}$, respectively) on the other hand were also very significant. Comparison with the values for the overall population shows that the tuned cells represent the outliers with respect to response to slow, and low-pass cells the outliers with respect to upper cutoff and optimal speed.

Tuning width could not be compared because for many curves it was undefined. Therefore we compared the average tuning curves for the three speed selectivity types, tuned, broadband, and low-pass cells with the use of the same procedure as Maunsell and Van Essen (1983). Responses for each polarity were normalized with respect to the maximum response, and the speed yielding the highest response (e.g., 4 deg/s in Fig. 2) was considered the optimum speed. Optimum speeds were aligned and data points on either side averaged. For most cells there was a response to both light and dark bars, and thus both sets of data points contributed to the average tuning. The results are shown in

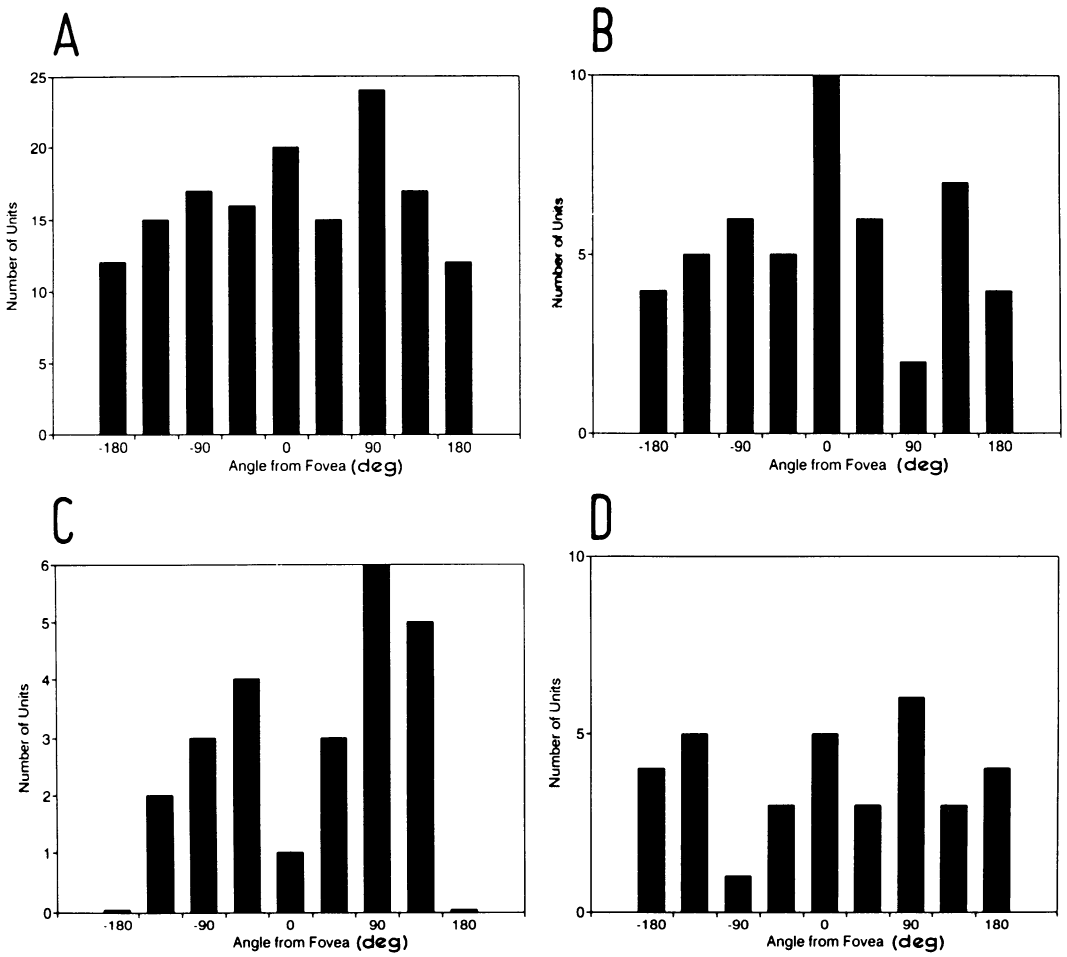

FIG. 11. Directional bias of middle temporal cells: the distribution of angular differences between the preferred direction (PD) and the direction linking the fixation point to the receptive-field center is plotted for the overall population (*A*, $n = 147$), the tuned cells (*B*, $n = 49$), the broadband cells (*C*, $n = 28$), and the low-pass cells (*D*, $n = 32$). Clockwise deviations of the PD from the centrifugal direction were plotted as positive values for the left hemifield and negative values in the right hemifield. Data corresponding to the extreme classes were plotted twice.

Fig. 9. The most important point to note about these average curves is their tuning width, which can be appreciated by the intersection with the half-maximum level. Indeed all these curves will look peaked because they were obtained by aligning the optimal responses. The average tuning of tuned cells (Fig. 9*A*) is indeed very sharp. Normalized response decreases to half maximum for less than an eightfold decrease in speed, and less than a fourfold increase in speed, yielding a tuning width of <30. The average tuning curve for broadband cells (Fig. 9*B*) is much broader than that of tuned cells. In fact, no tuning width can be determined for this average curve because average normalized response still exceeds 50% even at speeds 64 times slower than the optimum. The average tuning was also broader for low-pass cells (Fig. 9*C*) than for tuned cells, although the difference between the two types is less apparent because the speed normalization, to a certain extent, masks the selectivity for slow speeds characteristic of low-pass cells. Still the average tuning of low-pass cells is clearly wider than that of tuned cells because an eightfold increase is required to decrease the response to 50%, and an eightfold decrease in speed still yields normalized responses of 68%. Unfortunately, only two low-pass cells contributed to the datapoints at $^1/_{16}$ of optimal speed, but the average response for these two cells was in fact higher than the average response at $^1/_8$ of optimal speed. The differences in average curves between tuned cells on one hand, and low-pass and broadband cells on the other, reached statistical significance at many relative speeds (Fig. 9). Thus the average tuning curves, which are based on the raw data, emphasize the distinction between tuned units and the other two types.

There were also small differences in responsiveness and direction selectivity among the speed types. The response levels of the four groups were similar. The median maximum response (averaged for light and dark bars) was 39 spikes/s for low-pass cells, 38 spikes/s for broadband cells, 48 spikes/s for tuned cells, and 47 spikes/s for mixed cells. There was a steady increase in the proportion of cells responding very vigorously (>60 spikes/s) from low-pass (13%) to tuned cells (40%), the other two categories falling between these extremes. The difference in proportion of vigorous responses between lowpass and tuned cells was significant ($\chi^2 = 6.74$, $P < 0.01$).

The distributions of direction indexes of the different types are given in Fig. 10. About 60% of the tuned and low-pass cells have an MDI exceeding 80, compared with 45% of the broadband cells and the mixed cells. With respect to the PDI, ~65% of the tuned and broadband neurons have a PDI exceeding 90, compared with 55% of the low-pass and the mixed cells. Thus at the optimal speed the broadband and tuned cells are somewhat more directional than low-pass cells, perhaps because the optimal speed is faster in the former cells. However, the broadband cells do not sustain the direction selectivity over the full extent of their response range so much, compared with tuned and low-pass cells, which operate over a more narrow range of speeds. This is in fact quite apparent from Fig. 8. In almost all neurons, there is a distinct tendency for the direction

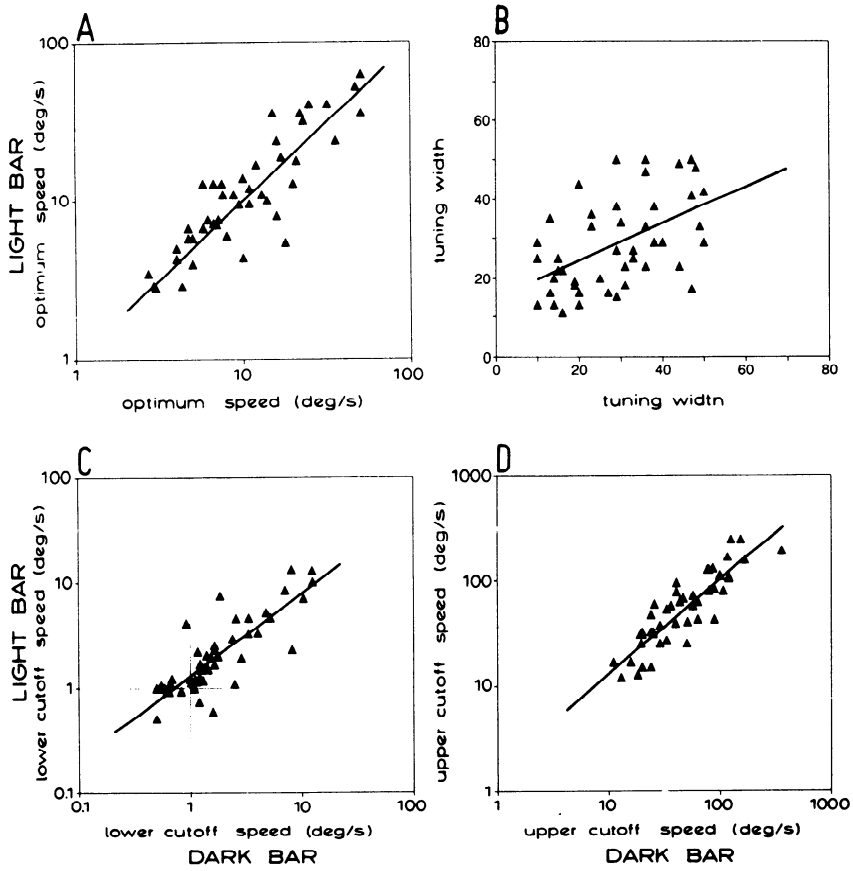

FIG. 12. Comparison of speed characteristics of tuned cells for light and dark bars ($n = 46$): optimum speed (*A*), tuning width (*B*), lower cutoff speed (*C*), and upper cutoff speed (*D*). Correlation coefficients were 0.84 (*A*), 0.47 (*B*), 0.83 (*C*), and 0.88 (*D*). Equations of linear regression are $y = 0.01 + x$ (*A*), $y = 16 + 0.42x$ (*B*), $y = 0.12 + 0.77x$ (*C*), and $y = 0.27 + 0.88x$ (*D*).

selectivity to decrease at slow speeds. In the broadband cells, however, there is an additional tendency to be less direction selective at the fastest speeds to which the cell is responsive. These results are completely compatible with the hypothesis that direction selectivity arises from spatiotemporal interactions operating for an optimal spacing and optimal delay, as many models suppose.

It has been reported by Albright (1989) that MT cells with RFs located >12° from the fixation point exhibit a directional bias. This is to say that for these neurons the PD aligns with the direction pointing radially from the fixation point to the RF center. For each cell of the sample, the angular difference between the direction from the fixation point to the RF center and the PD of the neuron was calculated. Figure 11*A* depicts the angular differences for all cells with an average (over L and D) MDI >50 (n = 136). The distribution is fairly uniform. Only 51/136 (38%) cells preferred directions within 67° from the centrifugal direction, exactly the proportion expected for a uniform distribution. This is in agreement with Albright's (1989) results because most of the neurons (85%) had RFs within 12° of the fixation point. There were, however, significant differences among speed selectivity types. The distribution of low-pass and tuned cells did not show any clear-cut bias, although 46% of the tuned cells preferred angles within 67° from the centrifugal direction. This is in striking contrast to broadband cells (Fig. 11*D*). The distribution of angular differences for broadband cells clusters around −90 and 90°, indicating a PD orthogonal to the centrifugal direction. The difference between the distributions of tuned and broadband cells was significant at the 1% level (χ^2 = 7.77, df = 1, $P < 0.01$).

Among the speed selectivity types, those with the steepest slopes in their curves are the tuned cells. This follows from their narrow tuning and strong responses. It has been shown that the slopes of tuning curves are the most important feature for discrimination (Vogels and Orban 1990). Hence characteristics of tuned cells might correlate with speed discrimination performance in primates. Figure 12*A* gives the correlation between optimal speeds for light and dark bars. The correlation is excellent as witnessed by the strong correlation coefficient (r = 0.84), much better than in the overall sample (Fig. 3*D*), and the nearness of the linear regression to the diagonal (slope = 1). Also the correlations of upper (r = 0.88) and lower (r = 0.83) cutoff speeds of tuned cells for light and dark bars were clearcut (Fig. 12, *C* and *D*). For comparison purposes, it is worth noting that the correlation for optimum and upper cutoff speeds of nontuned cells for light and dark bars was lower, the coefficients being 0.6 and 0.77 for optimum and upper

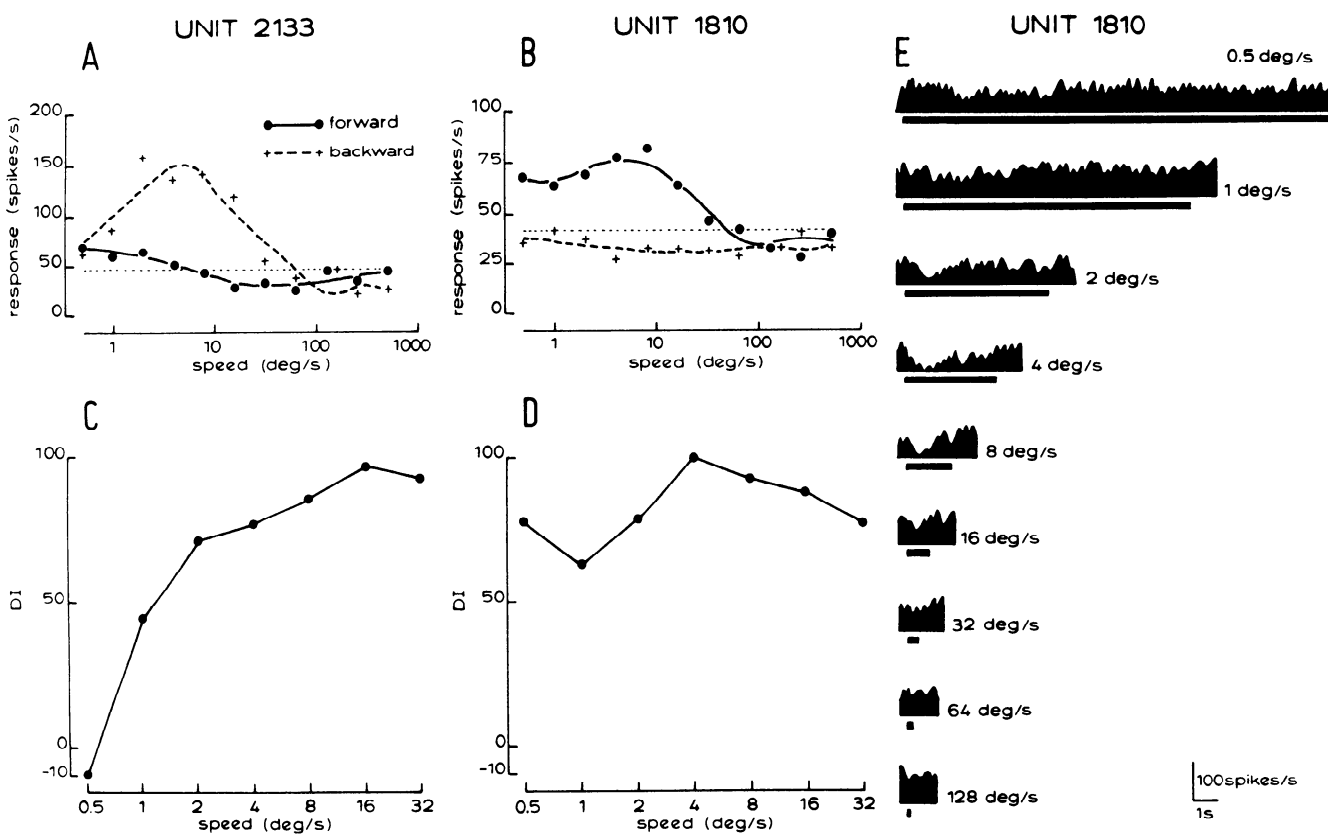

FIG. 13. *A* and *B*: Speed-response curve (dark bar stimulation) of a tuned cell (*A*) and of a low-pass cell (*B*). *C* and *D*: direction index (net DI) plotted as a function of speed for these units (*unit 2133, C, unit 1810, D*). A negative DI indicates a reversal of preferred direction. *Cell 1810* had a DI >50 for all speeds but was most direction selective at 4 deg/s. This was due to the strong inhibition at this speed in the nonpreferred direction (NPD) as shown in *E*. Histograms in *E* show the responses of *cell 1810* to movement in the NPD from 0.6 to 128 deg/s. Inhibition is seen from 2 to 16 deg/s. *Cell 1810* was recorded in layer 6, *cell 2133* in layer 5. The mean direction index (MDI) of *cell 1810* was 96 for the dark bar and 71 for the light bar. For *cell 2133* the values were 84 and 83, respectively. Same conventions as in Fig. 5.

cutoff, respectively. The correlation for tuning width of tuned cells (Fig. 12*B*) was somewhat less ($r = 0.51$, slope = 0.47), although median values were similar (29 and 27 for dark and light bar, respectively). Given these close correlations, these four characteristics were averaged over light and dark bars to describe the behavior of the cell. There was no correlation ($r = 0.005$) between the average tuning width and average optimal speed of tuned cells.

Changes in direction selectivity with speed

In many cortical areas of cat and monkey, direction selectivity depends on speed (Movshon 1975; Orban et al. 1981b, 1986). To analyze the dependence of direction selectivity on speed, we calculated the DI for every speed for which there was a significant response. This is shown for a tuned cell in Fig. 13, *A* and *C*. As speed increases, the DI rises steeply and then increases more gradually up to 16 deg/s. The initial rapid increase in the DI was due to an increase in response in the PD, whereas the minor increase following was due to a decrease in response in the NPD. Figure 8 shows that the decrease in DI at slow speed to be in fact a very general finding. The exact balance between increased facilitation and increased inhibition with increasing speed depended on the type of speed selectivity curve. Figure 8 also shows that in some cells there is a decrease in direction selectivity at faster speeds.

To capture the changes in direction selectivity with speed, we prepared speed-DI curves, as in Fig. 13*C*, for each cell with an average MDI exceeding 50, and calculated the distribution of DIs for each speed. The result is shown in Fig. 14*A*. This average curve shows that direction selectivity is maximal at a medium speed, 8–16 deg/s, and decreases on either side, yielding a tuned function. Notice that the decrease is more steady and more regular at the slow end than at the fast end, because fewer cells contribute to the fast end than to the slow end. Comparison of the two average curves in Fig. 14 shows that the speed-DI curve is shifted to the right of the SR curve. Indeed, the optimum of the average SR curve is 4–8 deg/s. This curve was quite similar whether only the cells with an average MDI exceeding 50 were considered, or whether all cells were taken into account. Thus the limiting factor of the direction selectivity at the population level is the loss of direction selectivity of individual cells at the slow speeds, and the loss of responsiveness of the neurons at the fast speeds.

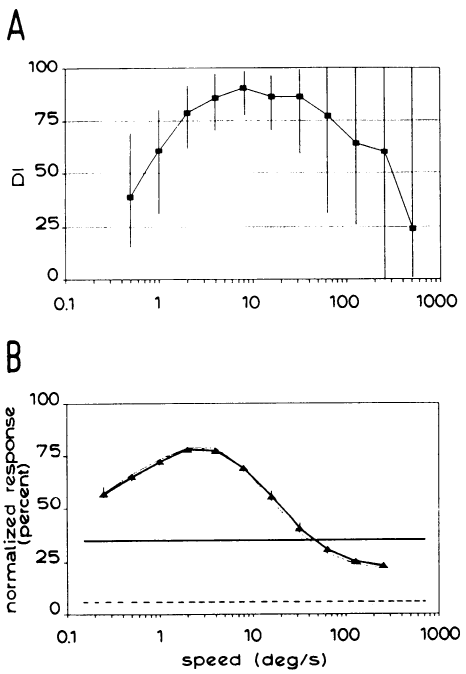

FIG. 14. Average speed direction index curve (*A*) and normalized response (*B*) for the total sample ($n = 147$). Medians and quartiles are indicated. In *B*, all cells contributed to each data point. In *A*, only cells with an average mean direction index (MDI) >50 and giving a significant response at a given speed contributed to this speed, therefore the number of cells contributing to a speed was unequal: 119 at 0.5 deg/s; 129 from 1 to 8 deg/s; 124, 102, 71, 43, 21, and 11 at 16, 32, 64, 128, 256, and 512 deg/s, respectively. Stippled line in *B* indicates the average response for cells with average MDI >50. Horizontal lines in *B* indicate average spontaneous activity (solid line, significance level; stippled line, mean level).

TABLE 4. *Distribution of speed selectivity type by layer*

	Class					
Layer	LP	BB	TU	MX	UC	Total
2–3	12 (28)	8 (19)	12 (28)	7 (16)	4 (9)	43 (100)
4	8 (21)	6 (15)	12 (31)	13 (33)	0 (0)	39 (100)
5	10 (30.5)	4 (12)	10 (30.5)	9 (27)	0 (0)	33 (100)
6	2 (6)	10 (31)	15 (47)	3 (10)	2 (6)	32 (100)
Total	32 (22)	28 (19)	49 (33)	32 (22)	6 (4)	147 (100)

Values shown are medium; numbers in parentheses are percentages. MX, mixed; other abbreviations, see Table 2.

In fact, the changes in direction selectivity with speed might still be underestimated in the curve of Fig. 14*A*. Indeed the DI and derived quantities such as MDI, based on maximum firing rate, do not take into account inhibition in the NPD. This is possible only for DIs based on average firing rate. Average firing rate can be less than the spontaneous firing rate and yield DIs exceeding 100. In a few cells with high spontaneous activity and strong inhibition in the NPD, we could directly observe the changes in inhibition in the NPD. The cell shown in Fig. 13, *B*, *D*, and *E*, is an example. *Cell 1810* was classified as low pass, and the SR curve for the dark bar is shown. The response levels change little between 0.5 and 16 deg/s, for both the PD and the NPD. Consequently, the net DI changes little with speed and exceeds 60 at all speeds (Fig. 13*D*). However, inspecting the PSTHs at the different speeds (Fig. 13*E*) for the NPD clearly shows that inhibition was present at the middle speeds, especially at 4 and 8 deg/s. In contrast, little or no inhibition was noticed at the two slowest speeds. Thus this is direct evidence that inhibition in the NPD increases with speed, contributing to the increase in direction selectivity as speed increases from very low values. It also indicates that the speed-DI curve does not fully represent the changes in direction selectivity with speed.

Laminar differences in speed and direction selectivity

The laminar difference in speed selectivity and direction selectivity was small. Table 4 gives the proportions of the

TABLE 5. *Laminar distribution of direction selectivity*

Layer	Direction Index*	
	MDI	PDI
2–3	88 (62–97)†	96 (79–100)
4	80 (62–88)	95 (73–100)
5	81 (66–88)	93 (85–100)
6	87 (68–92)	96 (82–100)

Numbers in parentheses are ranges. MDI, mean direction index; PDI, peak direction index. * Averaged over light and dark bars. † Median (1st and 3rd quartile).

different speed selectivity types as a function of cortical layer. Proportions of speed types are close to the overall proportion in all laminae (Table 4). The laminar showing the greatest deviation from the average is perhaps layer 6, which contains more broadband and tuned cells and fewer low-pass cells than other layers. Likewise, the speed characteristics were very similar in all layers. Regardless of layer, median upper cutoff was close to 36 deg/s, the overall median value, although the median value in layer 6 (52 deg/s) was somewhat higher than the median value of the other layers (25 deg/s). The other characteristics were even more evenly distributed. Median response to slow was close to the overall median of 53% and median optimum speed close to the overall median of 5.5 deg/s. Tuning width was close to 30 in all layers.

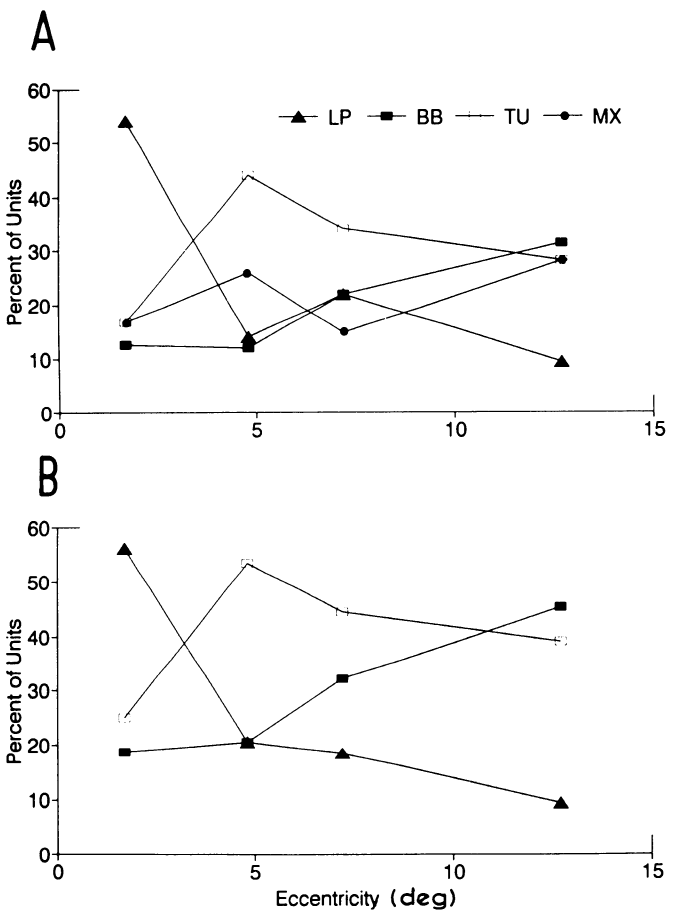

FIG. 15. Proportion of speed selectivity types plotted as a function of eccentricity: proportion of neurons (*A*) and proportion of curves (*B*). For size of the eccentricity classes, see Table 1.

TABLE 6. *Laminar distribution of the eccentricity dependence of proportion low-pass cells*

Eccentricity Group	Layer				Total
	2–3	4	5	6	
0–3°	50 (2)	38 (8)	62 (13)	100 (1)	54 (24)
Others	30 (37)	16 (31)	10 (20)	3 (29)	16 (117)
Total	31 (39)	21 (39)	30 (33)	7 (30)	23 (141)

Values are percentages; number of cells are in parentheses.

Direction selectivity tended to be even more uniform across laminae. The median MDI was close to 80 in all four laminae (Table 5) and the median PDI close to 95 in all layers (Table 5).

Changes in speed selectivity with eccentricity

Although the changes in speed selectivity were modest with laminar position, they were quite striking with respect to eccentricity. Figure 15 shows the proportion of cells of each speed selectivity type as a function of eccentricity. The proportion of low-pass cells decreases dramatically between the central class (0–3°) and the parafoveal class (3–6°) and then remains at a low level. The proportion of tuned cells is maximal (46%) parafoveally and decreases on either side, reaching 17% in the central class and 29% in the most peripheral class (>9°). Finally the proportion of broadband cells increases steadily with eccentricity, whereas the proportion of mixed cells hovers around 20% at all eccentricities. The same tendency is present if one examines the proportion of curves of a given type per eccentricity class (Fig. 15*B*) instead of the proportion of cells of a given type per eccentricity class. Low-pass curves dominate centrally, broadband curves peripherally, and tuned curves parafoveally. Thus the changes observed are not an artifact arising from the combination of light and dark bar responses in defining cell types.

Neither can these changes with eccentricity be explained by biases in the laminar sampling as a function of eccentricity. Indeed, the differential representation of certain speed selectivity types as a function of eccentricity occurs in all layers as shown in Tables 6 and 7. Low-pass cells are overrepresented in the central eccentricity class compared with all other classes (Fig. 15*A*). We therefore calculated for each layer, the proportion of low-pass cells in the central

TABLE 7. *Laminar distribution of the eccentricity dependence of proportion tuned cells*

Eccentricity Group	Layer				Total
	2–3	4	5	6	
3–6°	34 (29)	40 (25)	38 (16)	63 (16)	42 (86)
Others	20 (10)	14 (14)	24 (17)	36 (14)	24 (55)
Total	31 (39)	31 (39)	30 (33)	50 (30)	35 (141)

Values are percentages; number of cells are in parentheses.

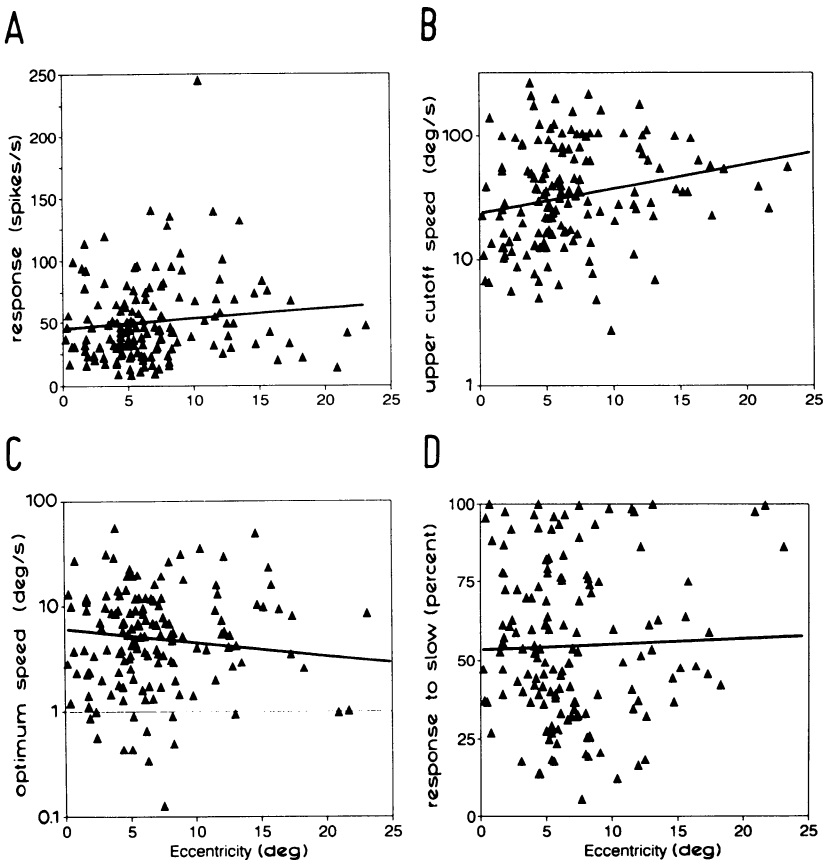

FIG. 16. Speed characteristics plotted as a function of eccentricity. *A*: maximum response. *B*: upper cutoff speed. *C*: optimum speed. *D*: response to slow. Regression coefficients were 0.1 (*A*), 0.02 (*B*), 0.05 (*C*), and 0.07 (*D*). Equations of linear regressions were $y = 46 + 0.82x$ (*A*), $y = 1.4 + 0.02x$ (*B*), $y = 0.79 - 0.01x$ (*C*), and $y = 54 + 0.16x$ (*D*).

class compared with the other eccentricity classes lumped together. The result is indicated in Table 6. In all layers there are large proportions of low-pass cells in the central eccentricity class and small proportions in the other classes. Similarly, tuned cells were most abundant in eccentricity class 3–6° and to a lesser extent in class 6–9°. Therefore, for each layer, we compared the proportion of tuned cells in the eccentricity group 3–9° with the proportion of tuned cells in the remaining eccentricity classes lumped together. The result is indicated in Table 7. In all layers, the proportion of tuned cells is larger in the 3–9° eccentricity group than in the remaining classes, the difference being largest in layer 4 and 6. Table 7 also indicates that for the eccentricity group 3–9° the proportion of tuned cells is somewhat larger in layer 6 (63%) than in the other layers. The same is true for the other eccentricity group. Thus the small increase in the proportion of tuned cells in layer 6 noticed in Table 4 might be genuine, rather than induced by the undersampling of the central eccentricity class in this layer (Table 1).

Although the proportions of speed selectivity types changed systematically with eccentricity, the speed characteristics did not change with eccentricity. Maximum response, upper cutoff, response to slow, and optimal speed were all independent of eccentricity (Fig. 16). The correlation coefficients of all four were close to zero, and the slopes of the linear regression lines were also near zero. This is

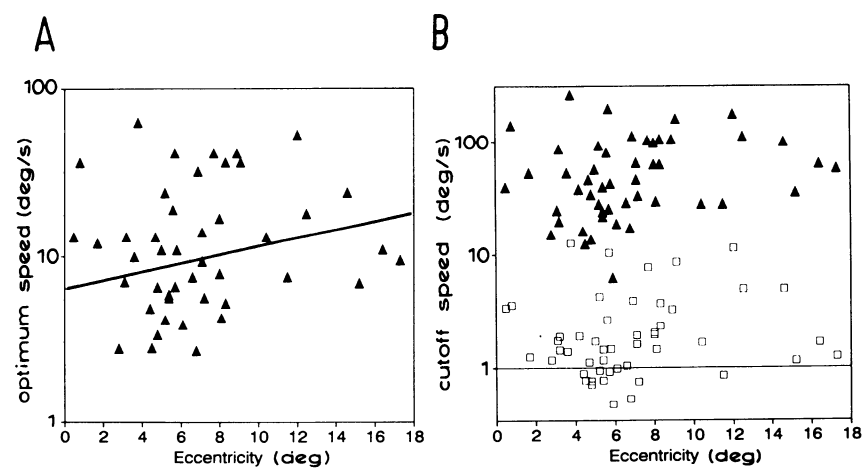

FIG. 17. Speed characteristics of tuned cells ($n = 49$) as a function of eccentricity: optimum speed (*A*) and cutoff speeds (*B*). In *A*, the correlation coefficient was 0.23 and the equation $y = 0.84 + 0.023x$. In *B*, triangles represent lower cutoffs and squares upper cutoffs. Notice that almost complete separation of the upper and lower cutoffs.

TABLE 8. *Eccentricity dependence of direction selectivity*

Eccentricity Class	Direction Index*	
	MDI†	PDI†
0–3°	81 (67–91)†	97 (79–100)
3–6°	79 (64–89)	92 (79–100)
6–9°	84 (71–88)	97 (92–100)
>9°	71 (44–90)	95 (78–100)

Numbers in parentheses are ranges. Abbreviations, see Table 5. * Averaged over light and dark bars. † Median (1st and 3rd quartile).

confirmed by the analysis of median values of the characteristics for the two extreme eccentricity classes. There was a small but nonsignificant increase in response level from a median value of 37 spikes/s to a median of 53 spikes/s. The change in response to slow was also small, the median value decreasing from 61 to 53%, as was the change in optimal speed: the median value increased from 3.4 to 5.6 deg/s. The only significant change was the increase in upper cutoff speed from a median of 15.3 to 38.5 deg/s. This change was significant at the 0.5% level. These results show that the changes in the proportion of speed selectivity types with eccentricity cannot be accounted for by changes in speed characteristics, underscoring the importance of the speed selectivity type classification.

Although the optimal speed did not depend on eccentricity for the overall population, it did so for the tuned cells (Fig. 17*A*). In these units, there is a weak correlation between optimal speed and eccentricity, as has been reported previously by Maunsell and Van Essen (1983). In fact, closer inspection reveals that cells tuned to slow speeds, <7 deg/s, occur only at eccentricities <8°. Similarly, small lower cutoff values, allowing discrimination at slow speeds, also occur at low eccentricities (Fig. 17*B*), although the eccentricity effect on lower cutoff was less than that on optimal speeds. In contrast, the fastest optima and the upper cutoff speeds changed little with eccentricity (Fig. 17, *A* and *B*). Thus the main eccentricity effect is a narrowing of the range of speeds over which tuned cells operate.

Changes in direction selectivity with eccentricity

There is a slight decrease in direction selectivity, as measured by the MDI, with eccentricity. Although the median average MDI is close to 80, for the central three eccentricity classes, the median average MDI falls below 70 for the peripheral class (Table 8). However, the PDI does not change with eccentricity. In all four eccentricity classes, the median average PDI is close to 95. The reason for this apparent discrepancy is probably the increase in broadband cells in the most eccentric class (>9°), because the direction selectivity is not maintained over the whole range of speeds to which these cells are responsive.

Figure 18 plots the median speed-DI curves for the four eccentricity classes. There is relatively little change in these

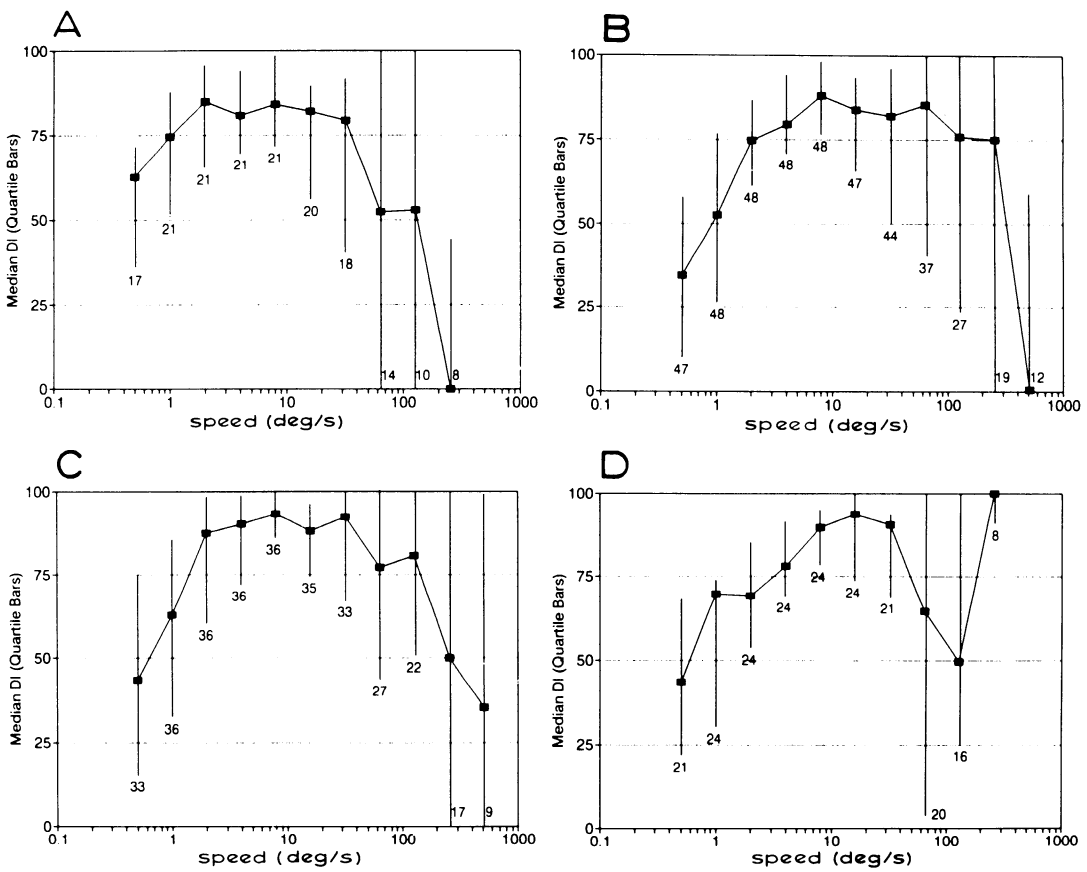

FIG. 18. Average speed direction index relationship for 4 eccentricity classes: 0–3° (*A*), 3–6° (*B*), 6–9° (*C*), and <9° (*D*). Same conventions as Fig. 13*A*. Numbers of cells contributing to each data point are indicated below the graphs.

curves with eccentricity at the fast end. However, there is some effect of eccentricity at the low end of the curves. The speed at which the speed-DI curve crosses the DI = 50 line is smaller (0.5 deg/s) for the central eccentricity class than for the other classes (1 deg/s). Thus direction selectivity is less sensitive to slowing of the bars in the center of the visual field than in more peripheral parts.

DISCUSSION

Comparison with previous studies

INVARIANCE. One of the most striking observations of our study is the remarkable correlation between speed characteristics for light and dark bars. All correlation coefficients were ≥ 0.7, whereas those for the direction indexes were close to 0.5. Invariance of speed tuning in MT cells has received little attention up to now, so that it is difficult to compare our results with those of others. A couple of studies, however, have been devoted to the invariance of direction tuning in MT neurons: Albright (1984) compared the direction tuning of MT neurons for moving light bars, moving light spots, and random dot patterns. In a subsequent study (Albright 1987), the same author went on to demonstrate an even greater degree of direction tuning invariance in MT with the use of isoluminant motion defined stimuli. In the 1984 study the correlation between direction indexes for bars and spots was only weak ($r = 0.38$), but the correlation of the direction indexes between random dot patterns and the two other stimuli was stronger (r close to 0.55). Thus the invariance we observed for direction selectivity agrees with that observed in the earlier studies, and the correlations for the speed characteristics are the more remarkable. It is worth noting that, for the tuned cells, the correlation between speed characteristics was even clearer than for the overall MT population: all correlation coefficients exceeded 0.8. Thus tuned cells will not only give responses that vary clearly with speed, but the changes with speed will also be very similar for moving light and dark bars.

SPEED SELECTIVITY. Optimum speed in the overall population ranged from 0.5 to 90 deg/s (median, 6 deg/s) and from 2 to 90 deg/s (median, 10 deg/s) among the tuned cells. This range is somewhat lower than what has been reported previously. Maunsell and Van Essen (1983) and Mikami et al. (1986a) reported a range from 2 to 256 deg/s with an average of 32 deg/s, whereas Rodman and Albright (1987), who explored a narrower range of speeds, reported a range of 5 to 150 deg/s with an average of 40 deg/s. It is noteworthy, however, that in an earlier study, Dubner and Zeki (1971) had reported that a substantial number of neurons in an area of the posterior bank of STS, which is now equated with MT, preferred slow speeds (1–5 deg/s). There are two probable reasons why we have found slower optimal speeds than those reported in the three most recent studies. First, we have observed cells with an extreme preference for slow speeds, the low-pass cells, mainly at eccentricities <3°. Few cells within this eccentricity range were included in the Maunsell and Van Essen study, which is the only one giving detailed information about eccentricity. Judging from their Fig. 8, only 8 out of 89 cells belonged to this eccentricity class. This cannot be the only explanation, because cells with slow optimal speed also occurred at higher eccentricities (Fig. 16*D*). The difference can hardly be attributed to the range of speeds explored. The range was more restricted in the Mikami et al. and Rodman and Albright study than in our study but was exactly the same in the Maunsell and Van Essen study. However, all three studies (Maunsell and Van Essen 1983; Mikami et al. 1986a; Rodman and Albright 1987) used average firing rate as criterion rather than maximum firing rate. Estimates of responses at slow speeds will be smaller with the use of average firing rate as criterion than with maximum firing rate as criterion (Orban 1984, 1991; Orban et al. 1981a). This can also be appreciated from Fig. 1. Average firing rate corresponds to maximum firing rate measured over a very large bin, and Fig. 1 shows that response to slow, even with maximum firing rate as criterion, decreases steadily as binwidth increases. The same two reasons probably also explain another difference between our study and that of Maunsell and Van Essen (1983). The proportion of tuned cells in Maunsell and Van Essen's study (82%) is much larger than in our study (44%). Indeed, only 20/109 cells in Maunsell and Van Essen's study (1983) did not fit the definition of a tuned cell.

Speed selectivity classification

The criteria used to classify SR curves are the same as those we used in previous studies of cat and monkey visual cortex (Duysens et al. 1982; Orban et al. 1981a, 1986). The present MT data, although showing that these criteria are acceptable, do not provide evidence for discrete classes. Thus the defining characteristics remain arbitrary. On the other hand, these classes differ in a number of important aspects, such as sharpness of tuning, distribution of preferred directions, and eccentricity dependence. Therefore we find this classification useful, especially to describe changes in speed selectivity with eccentricity that would be otherwise difficult to capture. At this point it is worth recalling that neither is there much evidence for discrete classes in the case of other, often made, distinctions such as direction-selective versus nonselective cells, end-stopped versus end-free cells, and oriented versus nonoriented cells.

Laminar position

Our study is the first to look at differences in speed and direction characteristics between cortical layers in MT. We observed very little difference in speed and direction selectivity among the different layers. This is in striking contrast to the results of another study from this laboratory investigating the modulation of direction selectivity for moving bars by moving noise fields (Lagae et al. 1989). In that study we found that neurons in which direction selectivity for a moving bar could be altered by a moving textured noise pattern belonged to either supra- or infragranular layers and not to lamina 4. Such modulatory effects on direction selectivity were attributed to antagonistic surrounds, such as those described earlier in the owl monkey (Allman et al. 1985). Since then, we have demon-

strated the presence of a surround more directly by preparing area summation curves. This has confirmed that surround mechanisms are weaker in layer 4 of area MT than in other laminae (Lagae et al. 1990).

Comparison with area V1

Superficially, the high proportion of tuned cells in MT might suggest a marked difference between MT and V1. Taking into account eccentricity and laminar position within V1 sharply reduces the contrast. Considering only small eccentricities, we compared MT speed profiles with those of V1 as reported in Orban et al. (1986). The proportion of low-pass cells was 80% in V1 compared with 55% in MT, whereas 10% of the cells in V1 and ~20% of the cells in MT were tuned or broadband cells. The difference is even smaller if one considers individual layers within V1. According to Orban et al. (1986) the proportion of low-pass cells is lowest in layers 4B and 6, which project to MT. Hence the speed selectivity of central visual field representation in MT is relatively similar to that in the V1 laminae projecting to MT. There is too much discrepancy at the large eccentricities between the Orban et al. (1986) study and this study to extend this comparison to other eccentricities.

Another similarity between V1 and MT parts representing central vision is the loss of direction selectivity at slow speeds that occurs at about the same speed (0.5 deg/s). Mikami et al. (1986b) have reported that the spatiotemporal range over which direction-selective interactions occur differs between V1 and MT but that this difference concerned only the maximum spatial interval, which determines the fastest speed at which direction selectivity is present, and not the slowest speed.

Finally, there is yet another similarity between V1 and MT. The proportions of low-pass and broadband cells show opposite eccentricity dependencies. This change corresponds to an increase in the upper cutoff speed for the nontuned cells. When the overall proportion of nontuned cells is large, as in V1, this is reflected in a correlation between eccentricity and upper cutoff speed. In MT this correlation was very weak (Fig. 16*B*) because of the large proportion of tuned cells. The replacement of low-pass cells by broadband cells with increasing eccentricity has been observed in all areas of cat and monkey cortex in which we have investigated speed selectivity: areas 17, 18 and 19 of the cat (Duysens et al. 1982; Orban et al. 1981a); area V1 of the monkey (Orban et al. 1986); and now MT. Thus the occurrence of a large proportion of low-pass cells in the part of cortical areas representing central vision is a hallmark of visual cortex. The reason for these observations is that space and time are interchangeable only for these cells. This means that only for these cells can spatial relations be deduced from the timing of discharges (Orban 1986, 1991), which is the only information present in the signal a cortical cell sends to its targets.

Functional implications

PURSUIT MOVEMENTS. The presence of a large proportion of low-pass cells in the part of MT subserving central vision fits perfectly with the report of Komatsu and Wurtz (1988), who reported pursuit cells active during pursuit in the foveal part of MT. Indeed slip velocities are small during pursuit, and thus pursuit cells must be sensitive to very slow speeds. It is thus likely that low-pass cells and pursuit cells represent the same population.

The changes in proportion of speed selectivity types with eccentricity shed a new light on the pursuit deficits caused by ibotenic lesions in different parts of MT. Tuned cells are ideally suited for estimation of target speeds and are therefore likely to play an important role in pursuit initiation. On the other hand, low-pass cells and not tuned cells are responsive to slow speeds and will remain active during the pursuit once the target is acquired. They could thus play an important role in maintenance of pursuit. Wurtz and coworkers (Dürsteler et al. 1987; Newsome et al. 1985) have observed two types of deficits after MT lesions. The deficit in acquisition manifests itself in amplitude errors in the saccade toward the target in the step-ramp paradigm, and in the undershooting of the eye speed during the initial 100 ms of the pursuit. This deficit is retinotopic and occurred both with lesions in peripheral MT and in foveal MT (Dürsteler et al. 1987; Newsome et al. 1985). We believe that this deficit is due to the loss of signals from tuned cells. Notice that, although the proportion of tuned cells is lower foveally than parafoveally, the number of tuned cells in the foveal representation will be large because of the magnification factor. The second deficit is nonretinotopic and is a maintenance deficit. It manifests itself as undershooting of the eye speed throughout the pursuit. This deficit occurred only after foveal MT lesions (Dürsteler et al. 1987). We believe this deficit is due to the elimination of the low-pass cells. Here, cortical magnification will amplify the changes in the number of low-pass cells within eccentricity. The nonretinotopic deficit was directional, and occurring only for pursuit of targets toward the side of the lesion, i.e., away from the lesioned visual hemifield. There is no explanation of the directionality in terms of the PD distributions of low-pass cells that had no clear bias (Fig. 11). A possible explanation could be that maintenance of pursuit depends on the balance of antagonistic signals between low-pass MT cells in the two hemispheres, just as has been postulated for the pretectal cells in the optokenetic nystagmus (OKN) (Hoffmann 1982). Lesion of foveal MT will upset this balance in such a way that the lesioned side can never dominate the other side yielding a deficit in only one direction.

MOTION PERCEPTION. Our results show that tuned cells have optimal speeds in the middle range of speeds, and that their range of optimal speeds narrows with eccentricity because of the absence of cells tuned to slow speeds. Given the linking hypothesis of Orban (1985), these results are in perfect agreement with the human data for speed discrimination published by Orban et al. (1985). These authors have shown that humans can make fine judgments of speed only at intermediate values, and that the range of speeds over which humans can make fine speed judgments narrows with eccentricity, because of a failure at slow speeds, and not at high speeds. Thus the range of fine speed judgments and of optima of MT tuned cells match closely, as predicted by the linking hypothesis stating that fine speed

judgment depends on tuned cells. However, the value of this observation is crucially dependent on the validity of cross-species comparison. In fact, Vandenbussche et al. (1991) have recently been able to show that monkeys, when tested in the same apparatus as humans, have exactly the same ability to make fine judgments in speed. The link between tuned MT cells and speed judgments is further supported by the recent reports of Vandenbussche et al. (1991) and of Merigan et al. (1991) that MT lesions impair severely speed discriminations in monkeys.

Our results also show that the direction selectivity of MT neurons as a population is bandpass, failing at slow speeds because of loss of selectivity of the cells and at fast speeds because of decreased responsiveness (Fig. 14). This is also in agreement with the observations of De Bruyn and Orban (1988), who showed that discrimination of opposite directions, an ability supposedly dependent on MT cells (Newsome and Paré 1988; Salzman and Newsome 1991), is most exquisite at intermediate speeds. It is only at these intermediate speeds (2–64 deg/s) that humans can discriminate opposite directions in motion of random dot patterns at low contrast (10%). Again it has been shown that humans and monkeys are similar in their abilities to judge opposite directions of motion (Newsome and Paré 1988; Newsome et al. 1989), lending validity to comparisons of monkey physiology with human perception.

We acknowledge the technical help of P. Kayenbergh, G. Vanparrijs, G. Meulemans, and Y. Celis. The authors are indebted to B. Gulyás for help during some of the initial experiments.

This work was supported by grants GOA 84/88 and RFO/A1/01 from the Ministry of Science to G. A. Orban. L. Lagae held a research fellowship of the National Research Council of Belgium (NFWO).

Address for reprint requests: G. A. Orban, Laboratorium voor Neuro-en Psychofysiologie K. U. Leuven, Campus Gasthuisberg, Herestraat, B-3000 Leuven, Belgium.

Received 18 February 1992; accepted in final form 17 September 1992.

REFERENCES

ALBRIGHT, T. D. Direction and orientation selectivity of neurons in visual area MT of the macaque. *J. Neurophysiol.* 52: 1106–1130, 1984.

ALBRIGHT, T. D. Isoluminant motion processing in macaque visual area MT. *Soc. Neurosci. Abstr.* 13: 1626, 1987.

ALBRIGHT, T. D. Centrifugal directional bias in the middle temporal visual area (MT) of the macaque. *Visual Neurosci.* 2: 177–188, 1989.

ALBRIGHT, T. D., DESIMONE, R., AND GROSS, C. G. Columnar organization of directionally selective cells in visual area MT of the macaque. *J. Neurophysiol.* 51: 16–31, 1984.

ALBUS, K. The detection of movement direction and effects of contrast reversal in the cat's striate cortex. *Vision Res.* 20: 289–293, 1980.

ALLMAN, J., MIEZIN, F. AND MCGUINNESS, E. Direction and velocity-specific responses from beyond the classical receptive field in the middle temporal visual area (MT). *Perception* 14: 105–126, 1985.

DE BRUYN, B. AND ORBAN, G. A. Human velocity and direction discrimination measured with random dot patterns. *Vision Res.* 28: 1323–1335, 1988.

DUBNER, R. AND ZEKI, S. M. Response properties and receptive fields of cells in an anatomically defined region of the superior temporal sulcus in the monkey. *Brain Res.* 35: 528–532, 1971.

DÜRSTELER, M. R., WURTZ, R. H., AND NEWSOME, W. T. Directional pursuit deficits following lesions of the foveal representation within the superior temporal sulcus of the macaque monkey. *J. Neurophysiol.* 57: 1262–1287, 1987.

DUYSENS, J., MAES, H., AND ORBAN, G. A. The velocity dependence of direction selectivity of visual cortical neurones in the cat. *J. Physiol. Lond.* 387: 95–113, 1987.

DUYSENS, J., ORBAN, G. A., VAN DER GLAS, H. W., AND DE ZEGHER, F. E. Functional properties of area 19 as compared to area 17 of the cat. *Brain Res.* 231: 279–291, 1982.

GALLYAS, F. Silver staining of myelin by means of physical development. *Neurol. Res.* 1: 203–209, 1979.

HOFFMANN, K-P. Cortical versus subcortical contributions to the optokinetic reflex in the cat. In: *Functional Basis of Ocular Motility Disorders,* edited by G. Lennerstrand, D. S. Zee, and E. L. Keller. Oxford, UK: Pergamon, 1982, Wenner Grn. Symp. Ser. 37, p. 303–310.

HUBEL, D. H. AND WIESEL, T. N. Receptive fields and functional architecture of monkey striate cortex. *J. Physiol. Lond.* 195: 215–243, 1968.

KOMATSU, H. AND WURTZ, R. H. Relation of cortical areas MT and MST to pursuit eye movements. I. Localization and visual properties of neurons. *J. Neurophysiol.* 60: 580–603, 1988.

LAGAE, L., GULYÁS, B., RAIGUEL, S., AND ORBAN, G. A. Laminar analysis of motion information processing in macaque V5. *Brain Res.* 496: 361–367, 1989.

LAGAE, L., RAIGUEL, S., XIAO, D., AND ORBAN, G. A. Surround properties of MT neurons show laminar organization. *Soc. Neurosci. Abstr.* 16: 6, 1990.

LAGAE, L., XIAO, D., RAIGUEL, S., MAES, H., AND ORBAN, G. A. Position invariance of optic flow component selectivity differentiates monkey MST and FST cells from MT cells (Abstract). *Invest. Ophthalmol. Visual Sci.* 32: 823, 1991.

MAES, H. AND ORBAN, G. A. STIMUL: stimulus control and multihistogram analysis of single neurone recordings. *Med. Biol. Eng. & Comput.* 18: 569–572, 1980.

MARCAR, V. L., RAIGUEL, S. E., XIAO, D., MAES, H., AND ORBAN, G. A. Do cells in area MT code the orientation of a kinetic boundary? *Soc. Neurosci. Abstr.* 17: 525, 1991.

MAUNSELL, J. H. R. AND VAN ESSEN, D. C. Functional properties of neurons in middle temporal visual area of the macaque monkey. I. Selectivity for stimulus direction, speed, and orientation. *J. Neurophysiol.* 49: 1127–1147, 1983.

MERIGAN, W. H., PASTERNAK, T., FERRERA, V., AND MAUNSELL, J. H. R. Permanent deficits in speed discrimination after MT/MST lesions in macaque monkeys. *Soc. Neurosci. Abstr.* 17: 8, 1991.

MIKAMI, A., NEWSOME, W. T., AND WURTZ, R. H. Motion selectivity in macaque visual cortex. I. Mechanisms of direction and speed selectivity in extrastriate area MT. *J. Neurophysiol.* 55: 1308–1327, 1986a.

MIKAMI, A., NEWSOME, W. T., AND WURTZ, R. H. Motion selectivity in macaque visual cortex. II. Spatiotemporal range of directional interactions in MT and V1. *J. Neurophysiol.* 55: 1328–1339, 1986b.

MOVSHON, J. A. The velocity tuning of single units in cat striate cortex. *J. Physiol. Lond.* 249: 445–468, 1975.

MOVSHON, J. A., ADELSON, E. H., GIZZI, M. S., AND NEWSOME, W. T. The analysis of moving visual patterns. In: *Pattern Recognition Mechanisms,* edited by C. Chagas, R. Gattass, and C. G. Gross. Vatican City: Pontificia Academia Scientiarium, 1985, p. 117–151.

NEWSOME, W. T., BRITTEN, K. H., AND MOVSHON, J. A. Neuronal correlates of a perceptual decision. *Nature Lond.* 341: 52–54, 1989.

NEWSOME, W. T. AND PARÉ, E. B. A selective impairment of motion perception following lesions of the middle temporal visual area (MT). *J. Neurosci.* 8: 2201–2211, 1988.

NEWSOME, W. T., WURTZ, R. H., DÜRSTELER, M. R., AND MIKAMI, A. Deficits in visual motion processing following ibotenic acid lesions of the middle temporal visual area of the macaque monkey. *J. Neurosci.* 5: 825–840, 1985.

NEWSOME, W. T., WURTZ, R. H., AND KOMATSU, H. Relation of cortical areas MT and MST to pursuit eye movements. II. Differentiation of retinal from extraretinal inputs. *J. Neurophysiol.* 60: 604–620, 1988.

ORBAN, G. A. *Neuronal Operations in the Visual Cortex. Studies of Brain Function,* edited by H. B. Barlow, T. H. Bullock, E. Florey, O. J. Grüsser, and A. Peters. Berlin: Springer-Verlag, 1984.

ORBAN, G. A. Velocity tuned cortical cells and human velocity discrimination. In: *Brain Mechanisms and Spatial Vision, NATO ASI Series, Series D: Behavioural and Social Sciences, No. 21,* edited by D. J. Ingle, M. Jeannerod, and D. N. Lee. Dordrecht, The Netherlands: Nijhoff, 1985, p. 371–388.

ORBAN, G. A. Processing of moving images in the geniculocortical pathway. In: *Visual Neuroscience,* edited by J. D. Pettigrew, K. J. Sanderson,

and W. R. Levick. Cambridge, UK: Cambridge Univ. Press, 1986, p. 121–141.

ORBAN, G. A. Quantitative electrophysiology of visual cortical neurons. In: *Vision and Visual Dysfunction,* edited by J. Cronly-Dillon and A. G. Leventhal. London: Macmillan, 1991, vol. 4, p. 173–222.

ORBAN, G. A., GULYÁS, B., SPILEERS, W., AND MAES, H. Responses of cat striate neurons to moving light and dark bars: changes with eccentricity. *J. Opt. Soc. Am.* A 4: 1653–1665, 1987.

ORBAN, G. A. AND KENNEDY, H. The influence of eccentricity on receptive field types and orientation selectivity in areas 17 and 18 of the cat. *Brain Res.* 208: 203–208, 1981.

ORBAN, G. A., KENNEDY, H., AND BULLIER, J. Velocity sensitivity and direction selectivity of neurons in areas V1 and V2 of the monkey: influence of eccentricity. *J. Neurophysiol.* 56: 462–480, 1986.

ORBAN, G. A., KENNEDY, H., AND MAES, H. Response to movement of neurons in areas 17 and 18 of the cat: velocity sensitivity. *J. Neurophysiol.* 45: 1043–1058, 1981a.

ORBAN, G. A., KENNEDY, H., AND MAES, H. Response to movement of neurons in areas 17 and 18 of the cat: direction selectivity. *J. Neurophysiol.* 45: 1059–1073, 1981b.

ORBAN, G. A., VAN CALENBERGH, F., DE BRUYN, B., AND MAES, H. Velocity discrimination in central and peripheral visual field. *J. Opt. Soc. Am.* A 2: 1836–1847, 1985.

PLANT, G. T. AND NAKAYAMA, K. Impaired motion perception following unilateral occipital damage (Abstract). *Invest. Ophthalmol. Visual Sci.* 32: 824, 1991.

RODMAN, H. R. AND ALBRIGHT, T. D. Coding of visual stimulus velocity in area MT of the macaque. *Vision Res.* 27: 2035–2048, 1987.

SAITO, H., TANAKA, K., ISONO, H., YASUDA, M., AND MIKAMI, A. Directionally selective response of cells in the middle temporal area (MT) of the macaque monkey to the movement of equiluminous opponent color stimuli. *Exp. Brain Res.* 75: 1–14, 1989.

SALZMAN, C. D. AND NEWSOME, W. T. Microstimulation of MT during an eight-alternative motion discrimination: directional tuning of the behavioral effect. *Soc. Neurosci. Abstr.* 17: 525, 1991.

TOOTELL, R. B. H. AND BORN, R. T. Architecture of primate area MT. *Soc. Neurosci. Abstr.* 17: 524, 1991.

VAINA, L. M., LEMAY, M., STRATTON, N., AND KEMPER, T. Speed discrimination and global motion perception in patients with unilateral posterior brain lesions. *Soc. Neurosci. Abstr.* 17: 8, 1991.

VANDENBUSSCHE, E., SAUNDERS, R. C., AND ORBAN, G. A. Lesions of MT impair speed discrimination performance in the Japanese monkeys (*Macaca Fuscata*). *Soc. Neurosci. Abstr.* 17: 8, 1991.

VAN ESSEN, D. C., MAUNSELL, J. H. R., AND BIXBY, J. L. The middle temporal visual area in the macaque: myeloarchitecture, connections, functional properties and topographic organization. *J. Comp. Neurol.* 199: 293–326, 1981.

VOGELS, R. AND ORBAN, G. A. How well do response changes of striate neurons signal differences in orientation: a study in the discriminating monkey. *J. Neurosci.* 10: 3543–3558, 1990.

YAMANE, S., MASKE, R., AND BISHOP, P. O. Direction selectivity of simple cells in cat striate cortex to moving light bars. II. Relation to moving dark bar responses. *Exp. Brain Res.* 57: 523–536, 1985.

ZEKI, S. M. Functional organization of a visual area in the posterior bank of the superior temporal sulcus of the rhesus monkey. *J. Physiol. Lond.* 236: 549–573, 1974.